EAVN Status Report
for the 2025A Semester

EAVN User Support Team (UST),
KASI, NAOJ, NGII, SHAO, XAO, YNAO, NGII, NARIT,
Ibaraki University, and Yamaguchi University

September 24, 2024

Major revisions since the 2024B semester

- Nobeyama 45-m and Kunming 40-m telescopes will not join the EAVN observations in the 2025A semester (Sections 2.2.3, 2.2.10, 3.1, and 3).

- Telescope time provided by Sejong is changed tentatively in the 2025A semester (100 hours → 50 hours; See Section 3.1.1 and Table 10).

- Available dates of the Sejong 22-m Telescope will be limited in the 2025A semester (Sections 2.2.11, 2.3.11, and 3.1.1).

- The selection criteria of one-year-long Proposals is changed (Section 3.5).

Contents

1 Introduction

This document describes the current observational capabilities as of 2024 Septemner, and available observing time of the East Asian VLBI Network (EAVN). EAVN is an international collaborative VLBI array operated by Korea Astronomy and Space Science Institute (KASI), National Astronomical Observatory of Japan (NAOJ), Shanghai Astronomical Observatory (SHAO; China), Xinjiang Astronomical Observatory (XAO; China), Yunnan Observatories (YNAO; China), and National Geographic Information Institute (NGII; Korea), and the National Astronomical Research Institute of Thailand (Public Organization; Thailand).

EAVN invites proposals for open-use observations to be carried out from January 16, 2025 to June 15, 2025 (2025A semester). The total observing time of 500 hours is provided for EAVN open-use operation to proposers, while the available machine time of each telescope is different between each other. Please refer to Table 10 in Section 3 for more details.

In the 2025A semester, EAVN is operated using 15 telescopes, all four 20-m telescopes of VERA, Takahagi 32-m, Hitachi 32-m, and Yamaguchi 32-m telescopes in Japan, all four 21-m telescopes of KVN including a newly constructed Pyeong-chang antenna since 2024B, and Sejong 22-m in Korea, Tianma 65-m, Sheshan 25-m, and Nanshan 26-m in China. **Two telescopes, Nobeyama 45-m and Kunming 40-m telescopes, do not join the EAVN observations in the 2025A semester due to the instrumental problems (Sections 2.2.3 and 2.2.10).** Figure 1 shows location of EAVN telescopes which participate in open-use observations of EAVN in the 2025A semester.

This status report summarizes general information about EAVN and the performance of each telescope/array, and how to prepare and submit proposals for EAVN. Please refer to the project overview of EAVN [4, 24], as well as the latest report for the overall performance of EAVN [6].

2 System

2.1 Array

In the 2025A semester, 15 radio telescopes (KVN 4 × 21 m, VERA 4 × 20 m, Takahagi 32 m, Hitachi 32 m, Yamaguchi 32 m, Tianma 65 m, Sheshan 25 m, Nanshan 26 m, and Sejong 22 m) are available for EAVN open use, as shown in Figure 1. From the 2024B semester, a newly constructed KVN Pyeongchang antenna is available for the EAVN common use observations on the shared-risk basis in the 2025A semester. **Nobeyama 45 m, and Kunming 40 m telescopes will not be available in the 2025A semester due to the instrumental problems (Sections 2.2.3 and 2.2.10).** Three observing frequencies, 6.7 (C-band), 22 (K-band) and 43 GHz (Q-band), are opened in the 2025A semester. **Dual-polarization observations at K-band and Q-band will be open for EAVN without any limitation for the maximum number of antennas in the shared-risk mode.** Details of the polarization observations will be described in this Status Report (subsections in Sections 2, 3, and 4.1).

Figure 1: Location of EAVN sites for the 2025A semester, including the Korea-Japan Correlation Center at KASI (Korea), Mizusawa VLBI observatory (NAOJ, Japan), and Shanghai Astronomical Observatory (China), overlaid on 'the Blue Marble' image (credit of the ground image: NASA's Earth Observatory).

KaVA (KVN and VERA Array) is a core array of EAVN, which consists of 8 antenna sites in VERA-Mizusawa, VERA-Iriki, VERA-Ogasawara, VERA-Ishigakijima, KVN-Yonsei (hereafter KYS), KVN-Ulsan (hereafter KUS), KVN-Tamna (hereafter KTN), and newly constructed KVN-Pyeongchang (hereafter KPC) on a shared-risk basis with 28 baselines in 2025A. Dual-polarization observations at K-band and Q-band are open for all the KaVA 8 antennas. The maximum baseline length of KaVA is 2270 km between VERA-Mizusawa and VERA-Ishigakijima stations, and the minimum baseline length is 130 km between the KYS and the KPC stations. The maximum angular resolution expected from the baseline length of KaVA is 4.0 mas for C-band, 1.2 mas for K-band and about 0.6 mas for Q-band. The maximum angular resolution is improved to be 1.8 mas at C-band and 0.55 mas at K-band for EAVN (the longest baseline of 5100 km for VERA-Ogasawara – Nanshan baseline for both bands), and that at Q-band was identical to that of VERA (0.63 mas for VERA-Mizusawa – VERA-Ishigakijima baseline) for the full-array of EAVN. The Sejong 22-m telescope of Korea (hereafter KSJ) has participated in the open-use program from the 2022A semester, resulting in making the minimum baseline length in EAVN of 120 km between the KSJ and the KYS stations. The dual-polarization observations with the KSJ become available from the 2024B semester on a risk-shared mode. The geographic locations and coordinates of EAVN antennas in the coordinate system of epoch 2009.0 are summarized in Table 1.

6

Figures 2 and 3 show examples of *uv* plane coverage for KaVA and EAVN, respectively. Figure 4 shows the elevation angle of each EAVN antenna as a function of hour angle.
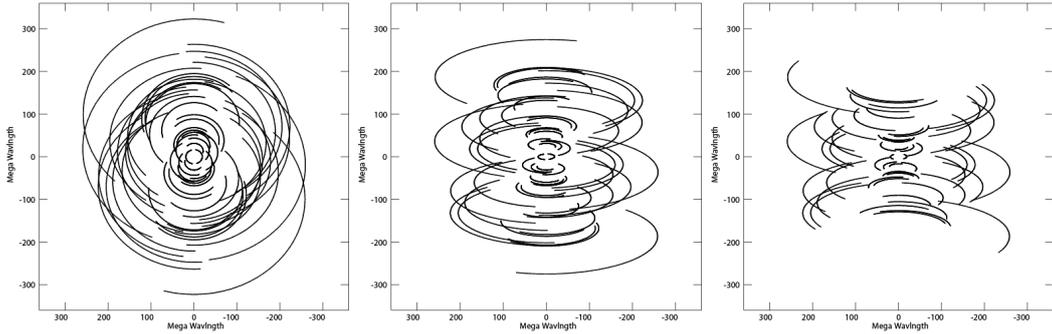
Figure 2: Examples of (u, v) coverage for a KaVA observation at Q-band with the source's declination of $+60°$ (left panel), $+20°$ (center panel), and $-20°$ (right panel). Total observation duration of 10 hours and the antenna's lower elevation limit of $15°$ are assumed for all cases.

The coordinates and averaged velocities of KaVA sites in Table 2 are predicted values at the epoch of January 1, 2018. Reference frame of these coordinates is ITRF2014. The rates of the coordinates of Mizusawa, Iriki, Ogasawara and Ishigakijima are the average value of change of the coordinates from April 16, 2016 to May 26, 2018, after the 2016 Kumamoto Earthquake ($M_j = 7.3$). The 2011 off the Pacific coast of Tohoku Earthquake ($M_j = 9.0$) brought the co-seismic large step and non-linear post-seismic movement to the coordinates of Mizusawa. Co-seismic steps of the coordinates of Mizusawa are $dX = -2.0297$ m, $dY = -1.4111$ m and $dZ = -1.0758$ m. The creeping continues still now, though decreased. The changes of coordinates by the post-seismic creeping are $dX = -1.2148$ m, $dY = -0.6402$ m and $dZ = -0.3042$ m in total from March 12, 2011 to January 1, 2020. Antenna positions of the KVN are regularly monitored by geodetic VLBI observations in collaboration with the VERA.
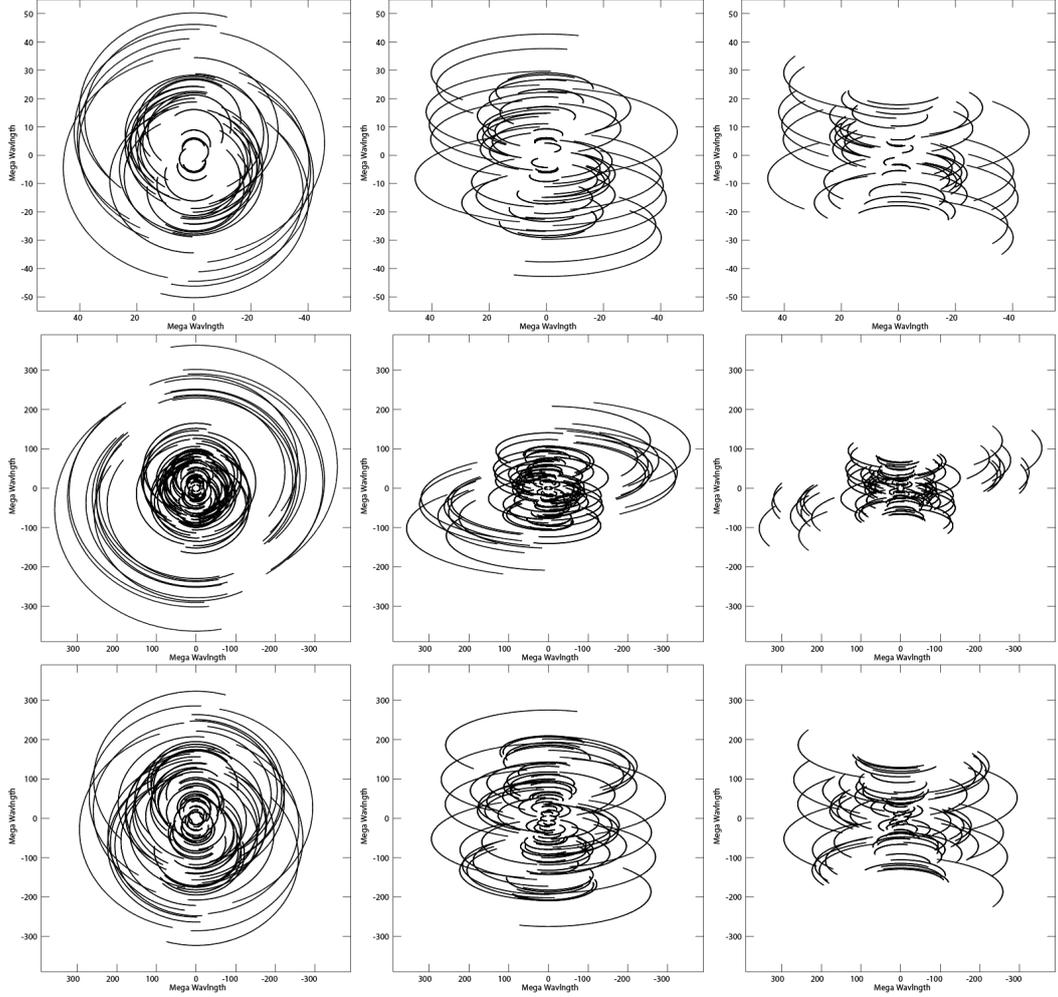
Figure 3: Examples of (u, v) coverage for an EAVN observation with full array configuration in the 2025A semester at C-band (upper panels), K-band (middle panels) and Q-band (lower panels) with the source's declination of $+60°$ (left panels), $+20°$ (center panels), and $-20°$ (right panels). Total observation duration of 10 hours and the antenna's lower elevation limit of $15°$ are assumed for all cases.
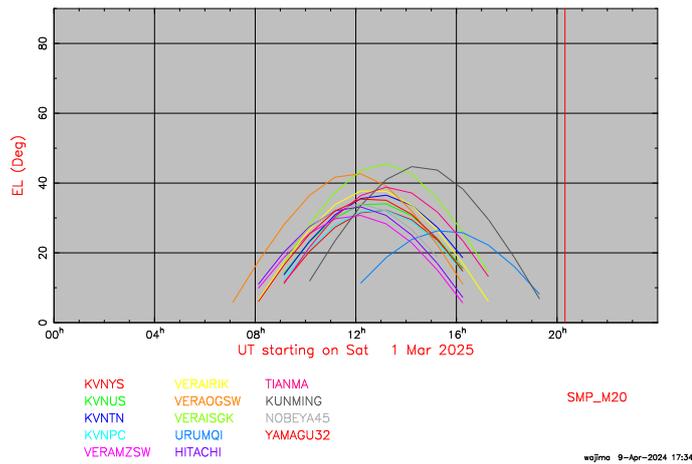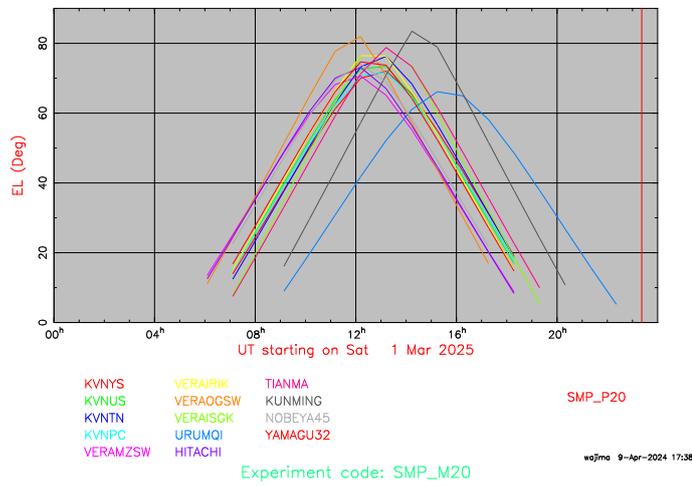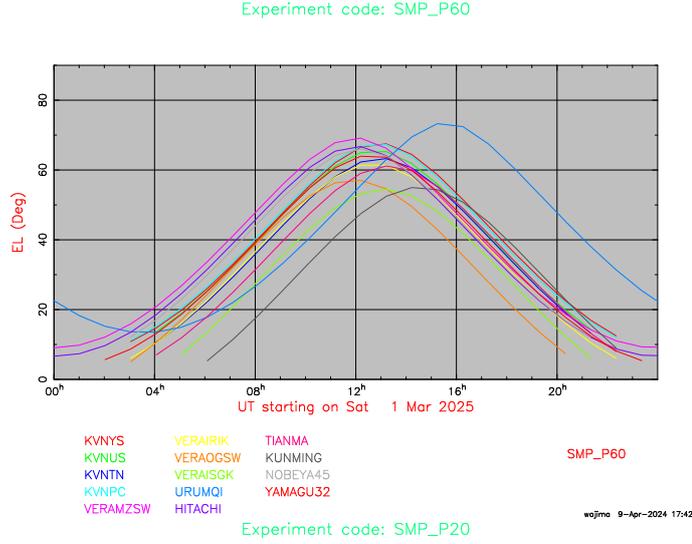
Figure 4: Examples of elevation angles of each EAVN antenna as a function of hour angle for the source's declination of +60° (top panel), +20° (middle panel), and −20° (bottom panel). Note that the elevation angle plot for Sheshan and Takahagi is almost identical to that for Tianma and Hitachi, respectively, because of their positional proximity.

Table 1: Geographic locations of each EAVN antenna.

Site	East Longitude [° ′ ″]	North Latitude [° ′ ″]	Ellipsoidal Height [m]	X [m]	Y [m]	Z [m]
Nobeyama[a]	138 28 21.2	35 56 40.9	1350	−3871025.4987	3428107.3984	3724038.7361
Takahagi[b]	140 41 41.0	36 41 54.5	117.1	−3961882.0160	3243372.5190	3790687.4570
Hitachi[b]	140 41 31.6	36 41 50.8	120.2	−3961789.1650	3243597.5310	3790597.7000
Yamaguchi	131 33 25.5	34 12 57.7	133	−3502544.587	3950966.235	3566381.192
Tianma[c]	121 08 09.4	31 05 31.6	49.2	−2826708.6380	4679237.0440	3274667.5330
Sheshan	121 11 58.8	31 05 57.0	29.4	−2831687.4306	4675733.4626	3275327.4941
Nanshan	87 10 40.4	43 28 15.6	2029.4	228310.1700	4631922.7550	4367064.0740
Kunming[c]	102 47 45.6	25 01 40.8	1974.0	−1281152.8860	5640864.4013	2682653.4578
Mizusawa[d]	141 07 57.3	39 08 00.7	116.6	−3857244.9731	3108782.9179	4003899.1695
Iriki[d]	130 26 23.6	31 44 52.4	573.6	−3521719.8813	4132174.6817	3336994.1132
Ogasawara[d]	142 12 59.8	27 05 30.5	273.1	−4491068.3826	3481545.2394	2887399.8018
Ishigakijima[d]	124 10 15.6	24 24 43.8	65.1	−3263995.2619	4808056.3902	2619948.6347
KYS[d]	126 56 27.4	37 33 54.9	139	−3042281.0290	4045902.6673	3867374.3313
KUS[e]	129 14 59.3	35 32 44.2	170	−3287268.8514	4023450.0317	3687379.9071
KTN[d]	126 27 34.4	33 17 20.9	452	−3171731.6818	4292678.5318	3481038.7880
KPC[f]	128 26 55.1	37 32 00.1	557	−3149228.7545	3966414.5854	3864840.1879
KSJ[g]	127 18 11.0	36 31 22.0	156	−3110079.9600	4082066.7340	3775076.8320

[a]The position was measured in late 2016.

[b]The position was measured in March 2020.

[c]The epoch of the coordinate is January 1, 2014.

[d]The epoch of the coordinates is September 20, 2019 (KaVA K-band Geodesy; r19262k).

[e]The epoch of the coordinates is August 29, 2022 (IVP measurement).

[f]The epoch of the coordinates is November 18, 2023 (IVP measurement).

[g]The epoch of the coordinates is October 2014.

Table 2: Station code and average velocity of each KaVA antenna.

Site	IVS2[a]	IVS8[b]	CDP[c]	ΔX [m/yr][d]	ΔY [m/yr][d]	ΔZ [m/yr][d]
Mizusawa	Vm	VERAMZSW	7362	−0.0433	−0.0138	−0.0047
Iriki	Vr	VERAIRIK	7364	−0.0159	−0.0049	−0.0098
Ogasawara	Vo	VERAOGSW	7363	0.0363	0.0242	0.0119
Ishigakijima	Vs	VERAISGK	7365	−0.0303	−0.0003	−0.0486
KYS	Ky	KVNYONSE		−0.0121	−0.0042	−0.0052
KUS	Ku	KVNULSAN		−0.0117	−0.0072	−0.0028
KTN	Kt	KVNTAMNA		−0.0169	−0.0012	−0.0024
KPC	Kc					

[a]IVS 2-characters code

[b]IVS 8-characters code

[c]CDP (NASA Crustal Dynamics Project) code

[d]The epoch of the coordinates is January 01, 2018. Average speed was obtained
from the VLBI data from January 01, 2018 to January 1, 2019.

2.2 Antennas

2.2.1 Brief Summary of VERA Antennas

All the telescopes of VERA have the same design, being a Cassegrain-type antenna on AZ-EL mount. Each telescope has a 20 m diameter dish with a focal length of 6 m, and with a sub-reflector of 2.6 m diameter. The dual-beam receiver systems are installed at the Cassegrain focus. Two receivers are set up on the Stewart-mount platforms, which are sustained by steerable six arms, and with such systems one can simultaneously observe two adjacent objects with a separation angle between 0.32 and 2.2 deg. The whole receiver systems are set up on the field rotator (FR), and the FR rotate to track the apparent motion of objects due to the earth rotation. Table 3 summarizes the ranges of elevation (EL), azimuth (AZ) and field rotator angle (FR) with their driving speeds and accelerations. In the case of single beam observing mode, one of two beams is placed at the antenna vertex (separation offset of 0 deg).

2.2.2 Brief Summary of KVN Antennas

The KVN antennas are designed to be a shaped-Cassegrain-type antenna with an AZ-EL mount. The telescope has a 21 m diameter main reflector with a focal length of 6.78 m. The main reflector consists of 200 aluminum panels with a manufacturing surface accuracy of about 65 μm. The slewing speed of the main reflector is 3 °/sec, which enables fast position-switching observations (Table 3). The sub-reflector position, tilt, and tip are remotely controlled and modeled to compensate for the gravitational deformation of the main reflector and for the sagging-down of the sub-reflector itself.

2.2.3 Nobeyama 45-m Telescope

While the Nobeyama 45 m telescope will not be available in the 2025A semester due to the problem in the hydrogen maser operated by the Mizusawa VLBI Observatory of NAOJ, detailed information is summarized in this section for references.

The Nobeyama 45-m Telescope (hereafter NRO45) is one of the largest millimeter radio telescopes in the world. It has a Cassegrain-Coudé optics. The paraboloidal main reflector consists of about 600 pieces of panels, each of which has a surface accuracy of about 60 microns, and the deviation of the whole antenna from an ideal paraboloid is about 90 microns. The sub-reflector has a diameter of 4 m with a convex hyperboloid surface, the position of which is computer-controlled to follow the moving focal point because the main reflector deforms as the elevation angle changes. The slewing speed of the telescope is $\sim$20°/min (i.e., 0.3°/sec). The (EL, AZ) driving ranges are also summarized in Table 3. According to the status report of NRO45, observers are required to conduct a pointing measurement and correction every 1 - 1.5 hours. In addition, it is appropriate to conduct a pointing measurement and correction every 30 minutes during the sunrise and sunset when the outside temperature changes drastically. The pointing accuracy above is achievable for wind speed of less than 4 m/s. It can be degraded if a wind velocity exceeds 10 m/s. Users are recommended to avoid observing targets located within 30 degrees from the Sun because the thermal deformation of the antenna degrades the pointing accuracy. Users who would like to

observe the Sun or targets near the Sun should take care of them. More details on the NRO45 can be found in the Nobeyama Radio Observatory official website [3].

2.2.4 Takahagi 32-m Telescope

The Takahagi 32-m Telescope (hereafter TAK32) has a shaped Cassegrain-Coude-type design with a 32-m diameter main reflector and a 2.9-m sub-reflector on Az-El mount. The telescope was constructed in 1992. Cryogenically-cooled receivers at 2 frequency bands (6 – 9 GHz and 21 – 25 GHz) are equipped. The surface accuracy of the main reflector is < 0.64 mm rms at the antenna elevation angle of 35 deg, and 1.6 mm at other antenna elevation angles. The surface accuracy of the sub-reflector is < 0.2 mm rms. The slewing rates of the main reflector is 0.07 deg/sec, as shown in Table 3. The tentative value of aperture efficiency of TAK32 is 30% at K-band (see Table 4; [25]). Although TAK32 can point to the El range of $5° \leq El \leq 88°$, we recommend to use at the El range of $15° \leq El \leq 85°$ because the pointing accuracy is not secured at $El \leq 15°$.

2.2.5 Hitachi 32-m Telescope

The Hitachi 32-m Telescope (hereafter HIT32) has a shaped Cassegrain-Coude-type design with a 32-m diameter main reflector and a 2.9-m sub-reflector on Az-El mount. The telescope was constructed in 1983. Cryogenically-cooled receivers at 2 frequency bands (6.5 – 12.5 GHz and 21 – 25 GHz) are equipped. The surface accuracy of the main reflector is < 0.64 mm rms at the antenna elevation angle of 35 deg, and 1.6 mm at other antenna elevation angles. The surface accuracy of the sub-reflector is < 0.2 mm rms. The slewing rates of the main reflector is 0.2 deg/sec, as shown in Table 3. The value of aperture efficiency of HIT32 is 60–75% at C-band (see Table 4; [25]). Although HIT32 can point to the El range of $5° \leq El \leq 88°$, we recommend to use at the El range of $15° \leq El \leq 85°$ because the pointing accuracy is not secured at $El \leq 15°$.

2.2.6 Yamaguchi 32-m Telescope

The Yamaguchi 32-m Telescope (hereafter YAM32) has a shaped Cassegrain-Coude-type design with a 32-m diameter main reflector and a 2.9-m sub-reflector on Az-El mount. The telescope was constructed in 1979. A cryogenically-cooled receiver for 6 and 8 GHz observation is equipped. The surface accuracy of the main reflector is < 0.64 mm rms at the antenna elevation angle of 35 deg, and 1.6 mm at other antenna elevation angles. The surface accuracy of the sub-reflector is < 0.2 mm rms. The slewing rates of the main reflector is 0.25 deg/sec, as shown in Table 3. The value of aperture efficiency of YAM32 is 60–70% at C-band (see Table 4).

2.2.7 Tianma 65-m Telescope

The Tianma 65-m Telescope (hereafter TMRT65) has a shaped Cassegrain-type design with a 65-m diameter main reflector and a 6.5-m sub-reflector on Az-El mount. The main reflector consists of 1008 aluminum panels deploying an active surface control system with 1104 actuators. The prime mirror achieves a surface accuracy of about 0.3 mm rms after compensating the gravitational deformation in real time by the active

surface control system. The secondary mirror has a surface error of 0.1 mm rms. A rotatable receiver cabin with the feeds covering frequency range from S-band (2 GHz) to Q-band is mounted at the Cassegrain focus, while the L-band (1.6 GHz) feed is off focus mount separately. The slewing rates of the main reflector are 0.5°/sec in azimuth and 0.3°/sec in elevation, as shown in Table 3. An overhead time of 10 seconds is recommended to settle the antenna on source.

Dual-beam receivers are installed in TMRT65 at both K- and Q-bands. These two beams have a fixed separation angle of 140 arcsec at K-band and 100 arcsec at Q-band. One of the beams is placed at the antenna focus for VLBI observations. The measured beam sizes (HPBW) are listed in Table 4.

2.2.8 Sheshan 25-m Telescope

The Sheshan 25-m Telescope (hereafter SHRT25) is a Cassegrain-type beam wave-guide antenna. The telescope has been in operation since 1987 and is located $\sim$ 6.1 kilometers from TMRT65. Current receiver system include a room-temperature C-band (6.7 GHz) receiver and a cooled S/X co-axis feed receiver. The main surface accuracy is 0.65 mm rms. The slewing speed are 1.0°/sec in azimuth and 0.6°/sec in elevation, as shown in Table 3.

2.2.9 Nanshan 26-m Telescope

The Nanshan 26-m Telescope (hereafter NSRT26) has a Cassegrain-type design with a 26-m diameter main reflector and a 3-m sub-reflector on Az-El mount. The telescope was constructed in 1993 with 25-m-diameter main reflector, while refurbishment of the telescope was completed in 2015 resulting in enlargement of the main reflector of 26 m and improvement of the antenna surface accuracy. Receivers at five frequency bands, L, S/X, C, K, and Q, are equipped, while the new Q-band cooled receiver had been installed in 2018 and now is under evaluation. The C-band receiver is available for the common-use observations in the 2025A semester on a shared-risk basis. The surface accuracy of main- and sub-reflectors are 0.4 mm rms and 0.1 mm rms, respectively. The slewing rates of the main reflector are 1.0°/sec in azimuth and 0.5°/sec in elevation, as shown in Table 3.

2.2.10 Kunming 40-m Telescope

While the Kunming 40-m telescope will not be available in the 2025A semester due to the problem in the telescope driving system, detailed information is summarized in this section for references.

The Kunming 40-m Telescope (hereafter KMRT40) has a Cassegrain-type design with a 40-m diameter main reflector and a 4.2-m sub-reflector on Az-El mount. The main reflector which diameter within 26 meters is solid aluminum panel and 26 to 40 meters is stainless steel mesh. The telescope was constructed in 2006 with only S/X receivers and upgraded in 2016 for installing a C-band receiver (4–8 GHz). The surface accuracy of solid aluminum panel and stainless steel mesh are 0.5 mm rms and 2.5 mm rms, respectively. The slewing rates of the main reflector are 1.0°/sec in azimuth and 0.5°/sec in elevation, as shown in Table 3.

2.2.11   Sejong 22-m Telescope

The Sejong Telescope (KSJ) is a Cassegrain-type 22-m diameter telescope built primarily for geodetic research, and can be observed at S, X, K and Q bands. Among them, S/X bands were designed for observation with the International VLBI Service (IVS), while K- and Q bands were designed for astronomical observation. The slewing speed of the antenna is $\sim 5°$/sec in both azimuth and elevation, which enables fast position-switching observations (see Table 3). Like KVN telescopes, the subreflector position, tilt, and tip are remotely controlled and modeled to compensate for the gravitational deformation of the main reflector and for the sagging-down of the subreflector itself. The pointing accuracy is $\sim 3''$ and $5''$ in the azimuth and elevation, respectively.

KSJ will not be operational from 2024 November 1 to 2025 February 28 for replacement of the receiver at 22 and 43 GHz.

Table 3: Driving performance of EAVN telescopes.

Driving axis	Driving range	Max. driving speed	Max. driving acceleration
Nobeyama			
AZ[a]	$-75° \sim 435°$	$0.3°$/sec	$0.3°$/sec^2
EL	$12° \sim 80°$	$0.3°$/sec	$0.3°$/sec^2
Takahagi			
AZ[a]	$11° \sim 349°$	$0.07°$/sec	$0.035°$/sec^2
EL	$5° \sim 88°$[c]	$0.07°$/sec	$0.035°$/sec^2
Hitachi			
AZ[a]	$2° \sim 358°$	$0.2°$/sec	$0.12°$/sec^2
EL	$5° \sim 88°$[c]	$0.2°$/sec	$0.12°$/sec^2
Yamaguchi			
AZ[a]	$2° \sim 358°$	$0.25°$/sec	$0.5°$/sec^2
EL	$5° \sim 85°$	$0.25°$/sec	$0.5°$/sec^2
Tianma			
AZ[a]	$-60° \sim 425°$	$0.5°$/sec	$0.27°$/sec^2
EL	$8° \sim 88°$	$0.3°$/sec	$0.16°$/sec^2
Sheshan			
AZ[a]	$-78° \sim 430°$	$1.0°$/sec	$0.5°$/sec^2
EL	$5° \sim 88.5°$	$0.6°$/sec	$0.28°$/sec^2
Nanshan			
AZ[a]	$-270° \sim 270°$	$1.0°$/sec	$0.5°$/sec^2
EL	$5° \sim 88°$	$0.5°$/sec	$0.5°$/sec^2
Kunming			
AZ[a]	$-270° \sim 270°$	$1.0°$/sec	$0.3°$/sec^2
EL	$8° \sim 88°$	$0.5°$/sec	$0.3°$/sec^2
VERA			
AZ[a]	$-90° \sim 450°$	$2.1°$/sec	$2.1°$/sec^2
EL	$5° \sim 85°$	$2.1°$/sec	$2.1°$/sec^2
FR[b]	$-270° \sim 270°$	$3.1°$/sec	$3.1°$/sec^2
KVN			
AZ[a]	$-90° \sim 450°$	$3.0°$/sec	$3.0°$/sec^2
EL	$5° \sim 88°$	$3.0°$/sec	$3.0°$/sec^2
KSJ			
AZ[a]	$-270° \sim 270°$	$5.0°$/sec	$5.0°$/sec^2
EL	$5° \sim 88°$	$5.0°$/sec	$5.0°$/sec^2

[a]The north is 0° and the east is 90°.

[b]Field rotator. FR is 0° when Beam-1 is at the sky side and Beam-2 is at the ground side, and CW is positive when a telescope is seen from a target source.

[c]Recommended EL range is 15°–85° for the Takahagi and Hitachi antennas.

Table 4: Aperture efficiency, beam size, and DPFU[a] of EAVN telescopes.

Telescope Name	D (m)	C-band (6.7 GHz)			K-band (22 GHz)			Q-band (43 GHz)		
		η_A (%)	HPBW (arcsec)	DPFU (K/Jy)	η_A (%)	HPBW (arcsec)	DPFU (K/Jy)	η_A (%)	HPBW (arcsec)	DPFU (K/Jy)
Nobeyama	45	—	—	—	61	72	0.351	53	39	0.305
Takahagi	32	—	—	—	30	100	0.087	—	—	—
Hitachi	32	60–75	270–280	0.197	—	—	—	—	—	—
Yamaguchi	32	60–70	310	0.197	—	—	—	—	—	—
Tianma	65	50–55	140	0.631	50	44	0.601	45	22	0.541
Nanshan	26	45–50	370	0.091	60	115	0.115	—	—	—
Sheshan	25	40–42	370	0.073	—	—	—	—	—	—
Kumming[b]	40	20–30	282	0.121	—	—	—	—	—	—
Mizusawa	20	50–55	530	0.060	48	139	0.055	50	74	0.057
Iriki	20	50–55	510	0.060	44	147	0.050	40	74	0.046
Ogasawara	20	50–55	515	0.060	43	142	0.049	42	74	0.048
Ishigakijima	20	50–55	530	0.060	44	142	0.050	42	72	0.048
KYS	21	—	—	—	65	130	0.082	67	66	0.084
KUS	21	62	420	0.078	71	127	0.088	68	66	0.085
KTN	21	—	—	—	71	128	0.089	67	63	0.084
KPC	21	—	—	—	75	123	0.094	73	59	0.092
KSJ	22	—	—	—	70	127	0.087	66	61	0.083

[a]: Degree Per Flux density Unit.
[b]: Low η_A due to problems with the feed, fixing.

2.2.12 Aperture Efficiency

The aperture efficiency of each VERA antenna is 50–55% at C-band, and about 40–50% at both K- and Q-bands (see Table 4). The measurements at C-band were based on the observations of 3C274 and Cyg-A (3C405) assuming that the flux densities are 58.7 and 237.4 Jy in C-band [20], respectively. For the K- and Q-bands, Jupiter is used for aperture efficiency measurements assuming the brightness temperature of 160 K in both K- and Q-bands. Due to the bad weather condition in some of the sessions, the measured efficiencies show large scatter. However, we conclude that the aperture efficiencies are not significantly changed compared with previous measurements. The elevation dependence of aperture efficiency for VERA antenna was also measured from the observations toward Cyg-A (3C405) and maser sources at C-band and K/Q-bands, respectively. Figure 6 shows the relation between the elevation and the aperture efficiency measured by integrating all the VERA stations data in C-band. The aperture efficiency at low elevation of ≤ 30 deg slightly increases while possible changes in the efficiency is less than about 20%. On the other hand, the gain curves for the VERA K- and Q-bands decrease only less than 10% at the low elevation of ≤ 20 deg. Concerning this elevation dependence, the observing data FITS file include a gain curve table (GC table), which is AIPS readable, in order to calibrate the dependence when the data reduction.

The aperture efficiency and beam size for each KVN antenna are also listed in Table 4. Aperture efficiency of KVN varies with elevation as shown in Figure 5. The main reflector panels of KVN antennas were installed to give the maximum gain at the elevation angle of 48°. The sagging of sub-reflector and the deformation of main reflector by gravity with elevation results in degradation of antenna aperture efficiency with elevation. In order to compensate this effect, KVN antennas use a hexapod to adjust sub-reflector position. Figure 5 shows the elevation dependence of antenna aperture efficiency of the KVN 21 m radio telescopes measured by observing Mars or Jupiter. By fitting a second order polynomial to the data and normalizing the fitted function with its maximum, we derived a normalized gain curve which has the following form:

$$G_{\mathrm{norm}} = A_0 EL^2 + A_1 EL + A_2, \tag{1}$$

where EL is the elevation in degree.

Aperture efficiency and beam size for non-KaVA telescopes are also summarized in Table 4. The values for NRO45 are based on the latest measurements in autumn 2017, where the Jupiter or the Mars was used as a reference source. The elevation dependence of the aperture efficiency is approximately constant over a range of El $\sim 25° - 50°$ at both K- and Q-bands.

In TMRT65, the main reflector panels were assembled to give the maximum surface accuracy at the elevation angle of 52°. The aperture efficiency goes down to less than 10% at low ($< 10°$) and high ($> 80°$) elevation angles, mainly due to the gravitational deformation. The active surface control system is used for compensating the gravitational effect at different elevation angles, making the gain curves as a constant over the elevation. Figure 7 shows the elevation dependence of the aperture efficiency at Q-band with or without the active surface control. The active surface control system is set 'ON' by default at K- and Q-band observations. To calibrate visibility amplitude, conversion factors from temprature (in unit of K) to flux density (in unit of Jy) are required. These factors, DPFU (Degree Per Flux density Unit), are also summarized

in Table 4.
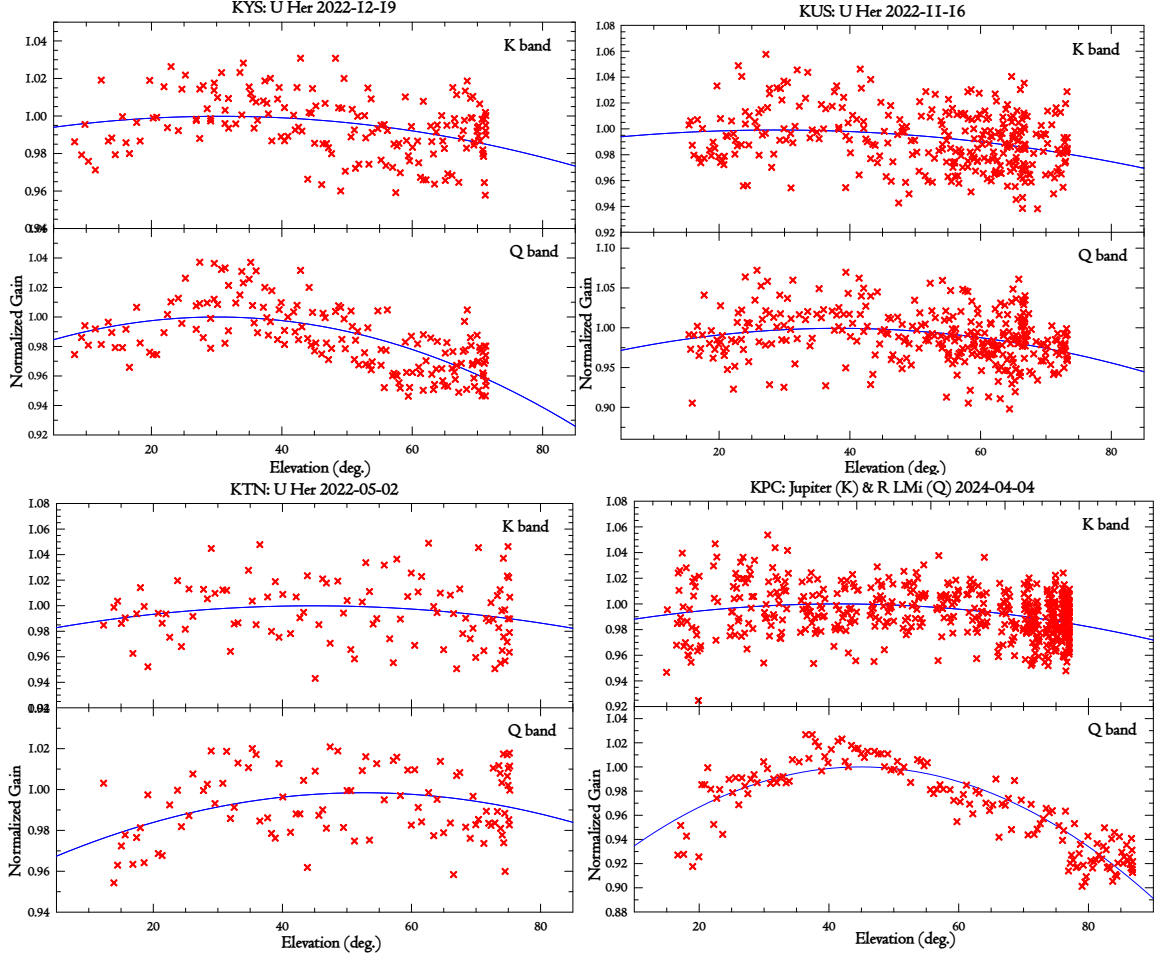
Figure 5: The elevation dependence of the aperture efficiency for KVN four antennas.

2.2.13 Beam Pattern and Size

Figure 8 upper panels shows the beam patterns for VERA at K-band. The side-lobe level is less than about -15 dB, except for the relatively high side-lobe level of about -10 dB for the separation angle of 2.0 deg at Ogasawara station. The side-lobe of the beam patterns has an asymmetric shape, but the main beam has a symmetric Gaussian shape without dependence on separation angle. Figure 9 shows the beam patterns for VERA Mizusawa and Ishigakijima stations at C-band (single-beam mode) measured via observing strong CH_3OH maser sources G 009.62+00.196 and W3-IRS5, which can be assumed as a point source, on 2017 Apr 5-8. Almost the similar side-lobe pattern is clearly seen in both stations and other VERA two stations as well. The measured beam sizes (HPBW) in C-, K- and Q-bands based on the data of the pointing calibration are also summarized in Table 4. The main beam sizes show no dependence on the dual-beam separation angle.

The optics of KVN antenna is a shaped Cassegrain type of which the main reflector and subreflector are shaped to have a uniform illumination pattern on an aperture plane. Because of the uniform illumination, KVN antennas can get higher aperture efficiency than value of typical Cassegrain type antenna. However, higher side-lobe
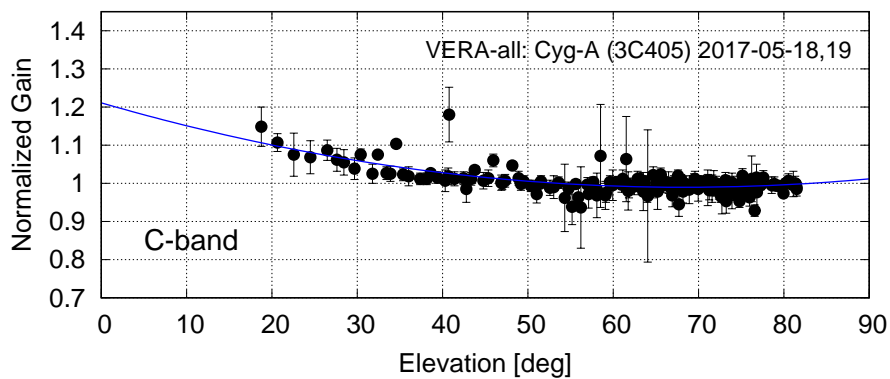
Figure 6: The elevation dependence of the aperture efficiency for VERA in C-band. This gain curve was measured on May 18 and 19, 2017 via observing Cyg-A (3C405) and integrating all the VERA stations data. The efficiency in this plot is relative value to the measurement at EL = 50°.
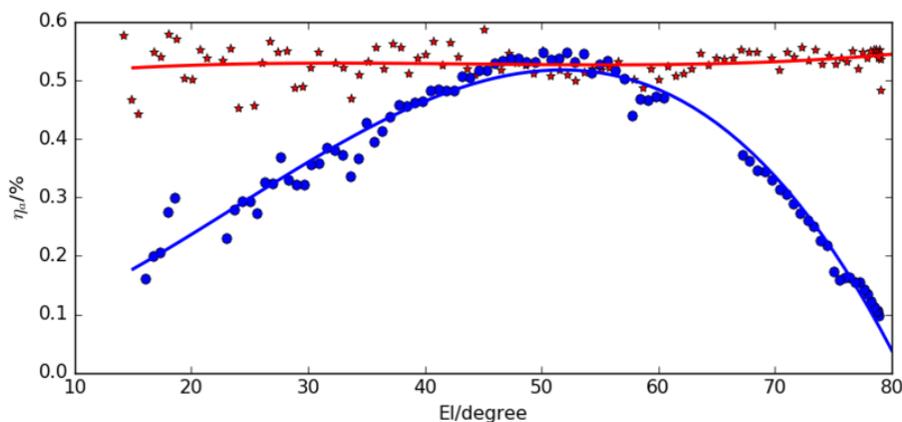
Figure 7: The elevation dependence of the aperture efficiency (η_{eff}) for TMRT65 at Q-band. The red and blue colors represent η_{eff} with or without the active surface control, respectively.

level is inevitable. OTF images of Jupiter at K- and Q-bands are shown in Figure 8. The map size is $12' \times 10'$ and the first side-lobe pattern is clearly visible. Typical side-lobe levels of KVN antennas are 13–14 dB.

19
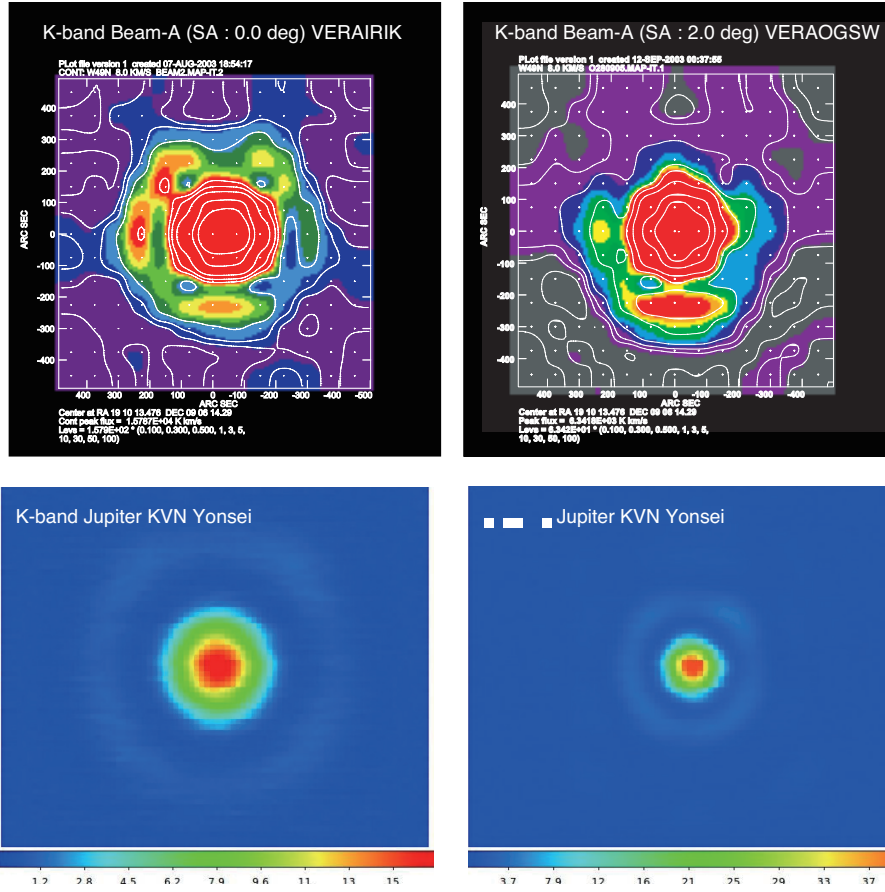
Figure 8: The beam patterns in the K-band for VERA (A-beam) Iriki with the separation angle of 0° (*Upper left*), Ogasawara with the separation angle of 2.0°(*Upper right*), and in K/Q-band for the KYS (*Lower left and right*). The patterns of VERA antennas were derived from the mapping observation of strong H_2O maser toward W49N, which can be assumed as a point source, with grid spacing of 75″. In the case of KVN antennas, the patterns were derived from the OTF images of Venus at K/Q-band.
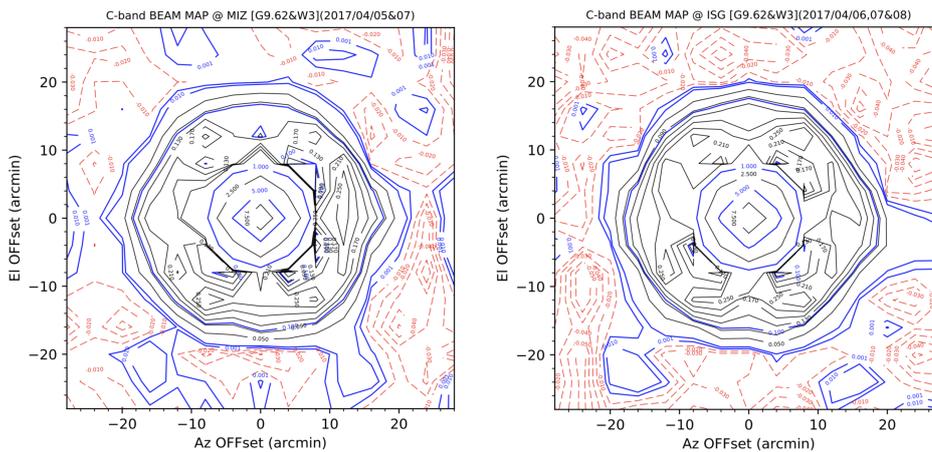
Figure 9: The beam patterns in C-band for VERA antennas (single beam) at Mizusawa and Ishigakijima stations. The patterns were derived from the mapping observation of strong CH_3OH masers toward G 009.62+00.196 and W3-IRS5, which can be assumed as a point source, with grid spacing of 4′ in 56′ × 56′ field. These observations were done in Apr 5–8, 2017.

2.3 Receivers

2.3.1 Brief Summary of VERA Receiving System

Each VERA antenna has the receivers for 5 bands, which are S (2 GHz), C (6.7 GHz), X (8 GHz), K (22 GHz), and Q (43 GHz) bands. For the open use, C-band, K-band and Q-band are open for observation in the single-polarization (LCP) mode. Observations of the dual-circular-polarization are also available for open use programs at K- and Q-bands. The low-noise HEMT amplifiers in the K- and Q-bands are enclosed in the cryogenic dewar, which is cooled down to 20 K, to reduce the thermal noise. On the other hand, both the amplifier and polarizer in C-band are operated at room temperatures. The range of observable frequency and the typical receiver noise temperature ($T_{\rm RX}$) at each band are summarized in Table 5 and Figure 10.

Table 5: Frequency range and T_{RX} of receivers at each EAVN telescope.

Band	Frequency Range [GHz]	$T_{\rm RX}$[a] [K]	Polarization
		Nobeyama	
K	21.5 − 23.8	∼ 85	LCP/RCP
Q	42.5 − 44.5	∼ 111	LCP
		Takahagi	
K	21.0 − 25.0	∼ 30	LCP/RCP
		Hitachi	
C	6.6 − 7.1	∼ 20	LCP/RCP
		Yamaguchi	
C	6.6 − 7.1	18	LCP/RCP
		Tianma	
C	4.0 − 8.0	∼ 20	LCP/RCP
K	18.0 − 26.5	16 − 35	LCP/RCP
Q	39 − 47	35 − 50	LCP/RCP
		Nanshan	
C	4.0 − 8.0	∼ 15	LCP/RCP
K	22.0 − 24.2	∼ 15	LCP/RCP
Q		(under evaluation)	
		Sheshan	
C	5.975 − 6.825	∼ 100	LCP/RCP
		Kunming	
C	4.0 − 8.0	∼ 20	LCP/RCP
		VERA	
C	6.3 − 7.0	80 − 100	LCP
K	21.5 − 23.8	30 − 50	LCP/RCP[c]
Q	42.5 − 44.5	70 − 90	LCP/RCP
		KVN	
C [b]	6.3 − 7.0	∼ 300	LCP
K	18 − 26	50 − 80	LCP/RCP
Q	35 − 50	50 − 80	LCP/RCP
		KSJ	
K	21.2 − 22.3	∼ 31	LCP/RCP
Q	42.1 − 43.7	∼ 86	LCP/RCP

[a] Receiver noise temperature.
[b] Only for the Ulsan antenna.
[c] RCP is used for the simultaneous K/Q band mode (see Section 4.5).

After the radio frequency (RF) signals from astronomical objects are amplified by
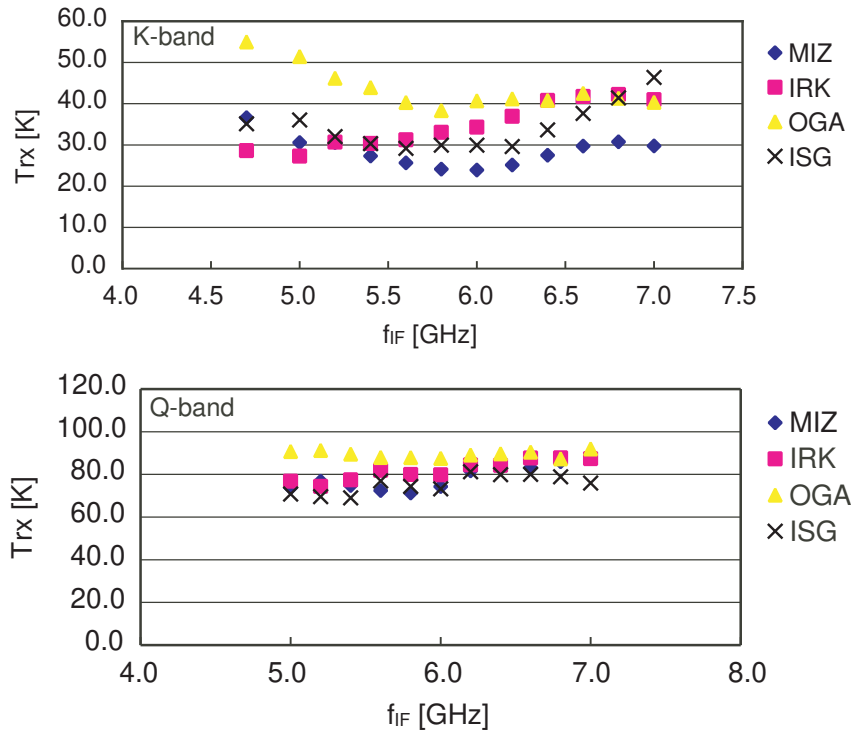
Figure 10: Receiver noise temperature for each VERA antenna. Top and bottom panels show measurements in the K- and Q-bands, respectively. Horizontal axis indicate an IF (intermediate frequency) at which T_{RX} is measured. To convert it to RF (radio frequency), add 16.8 GHz in K-band and 37.5 GHz in Q-band to the IF frequency.

the receivers, the RF signals are mixed with standard frequency signal generated in the first local oscillator to down-convert the RF to an intermediate frequency (IF) of 4.7 – 7 GHz. The first local frequencies are fixed at 16.8 GHz in K-band and at 37.5 GHz in Q-band. The IF signals are then mixed down again to the base band frequency of 0 – 512 MHz. The frequency of second local oscillator is tunable with a possible frequency range between 4 GHz and 7 GHz. The correction of the Doppler effect due to the earth rotation is carried out in the correlation process after the observation. Therefore, basically the second local oscillator frequency is kept to be constant during the observation. Figure 11 shows a flow diagram of these signals for VERA.

Figure 11: Flow diagram of signals from receiver to recorder for VERA.

2.3.2 Brief Summary of KVN Receiving System

The KVN quasi-optics are uniquely designed to observe 22, 43, 86 and 129 GHz band simultaneously [9], [10]. Figure 12 shows the layout of quasi-optics and receivers viewing from sub-reflector side. The quasi-optics system splits one signal from sub-reflector into four using three dichroic low-pass filters marked as LPF1, LPF2 and LPF3 in the Figure 12. The split signals into four different frequency bands are guided to corresponding receivers. Figure 13 shows a signal flows in the KVN system. The 22, 43 and 86 GHz band receivers are cooled HEMT receivers and the 129 GHz band receiver is a SIS mixer receiver. All receivers can receive dual-circular-polarization signals. The dual-circular-polarization mode is available for open use programs at K- and Q-bands. Among eight signals (four dual-polarization signals), four signals selected by the IF selector are down-converted to the input frequency band of the sampler. The samplers digitize signals into 2-bit data streams with four quantization levels. The sampling rate is 1024 Mega samples per second, resulting in a 2 Gbps data rate (2-bit × 1024 megabytes per second) and 512 MHz frequency bandwidth. In total, we can get 4 streams of 512 MHz bandwidth (2 Gbps data rate) simultaneously, which means that the total rate is 8 Gbps.

Figure 12: KVN multi-frequency receiving system [9], [10].

New wide-band VLBI backends, including OCTAD, Mark 6, and GPU spectrometers, are introduced for wide-band operation. They are indicated in the red box of Figure 13. The OCTAD consists of four analog-to-digital converters, digital signal processing modules, and a VDIF formatter. It digitizes four IF signals and performs signal processing for digital down-conversion and filtering. Combining OCTAD and ADS1K+Fila10G, all eight IF signals (four dual-polarization signals) can be obtained at the same time. The OCTAD has four 10 GbE outputs, with which we can get a maximum 32 Gbps aggregated data rate.

In mid-2023, the construction of the KPC Radio Telescope was completed. It has

Figure 13: Flow diagram of signals from receiver to recorder for the KVN.

been conducting test observations until recently, with most of the testing finished. The receiving system of the Pyeongchang Telescope has been developed as an compact and wideband receiver capable of simultaneous observations in the $18-230\,\text{GHz}$ band. For the K, Q, and W bands, a compact three-channel receiver (a.k.a., CTR, Compact Triple-band Receiver) was designed and manufactured in-house to simultaneously observe them. Figure 14 shows the CTR installed in the receiver room of the Pyeongchang Telescope and its structure.

Typical noise temperatures of K- and Q-bands are presented in Table 5. Since the calibration chopper is located before the quasi-optics as shown in Figure 12, the loss of quasi-optics contributes to receiver noise temperature instead of degrading antenna aperture efficiency. Therefore, the noise temperature in the table includes the contribution due to the quasi-optics losses.

2.3.3 Brief Summary of NRO45 Receiving System

While the Nobeyama 45 m telescope will not be available in the 2025A semester due to the problem in the hydrogen maser operated by the Mizusawa VLBI Observatory of NAOJ, detailed information is summarized in this section for references.

The NRO45 covers an observing frequency range of 20 – 116 GHz with multiple receivers. The VLBI backend system of the NRO45 is currently equipped at K-band and Q-band. Figure 15 illustrates a flow diagram of the VLBI receiving system in the NRO45. The observable RF range and typical receiver noise temperature for the receivers at K- and Q-bands are also summarized in Table 5. The received RF signals are down-converted into an IF range of 5 – 7 GHz, then the IF signals are mixed down to the another IF range of 400–2000 MHz, and finally filtered to the base bands of
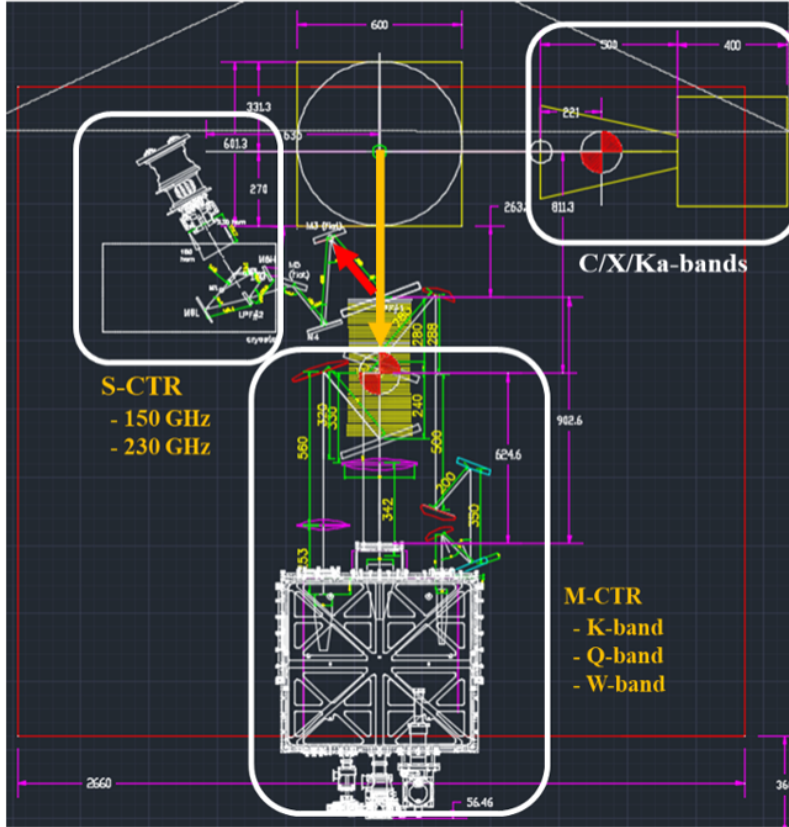
Figure 14: The CTR receiving system installed on the KPC.

512 –1024 MHz and 1024–1536 MHz in K- and Q-bands, respectively, which are the inputs to the A/D sampler. Because of the fixed frequencies of the first (16800 MHz) and second (4500 MHz) local oscillators and the bandpass filter (512–1024 MHz), the frequency range of the RF signal is fixed to 21812–22324 MHz for K-band. Only LCP signals are recorded in both K-band and Q-band (except for simultaneous K/Q band mode).

By default, one of the receivers at K- or Q-band can be selected by switching the mirrors in the optics in a few minutes manually. Since 2020B, K- and Q-band observations can be conducted simultaneously by inserting a perforated high-pass dichroic plate [19]. When using the dichroic plate, the gain of the Q-band signals may be reduced by 0.3 dB (in 2018 June), causing the rise of the system noise temperature by about 30 K in Q-band. In the case of the simultaneous K- and Q- band observations, RCP and LCP signals are recorded, respectively (See Table 27).

2.3.4   Brief Summary of TAK32 Receiving System

Figure 16 shows a flow diagram of the VLBI receiving system in TAK32. TAK32 covers an observing frequency range of 6 – 9 GHz and 21 – 25 GHz with two cryogenically-cooled receivers, while TAK32 joins in EAVN observations at only K-band in the 2025A semester.

The flow diagram of TAK32 is shown in Figure 16. The K-band receiver is cooled
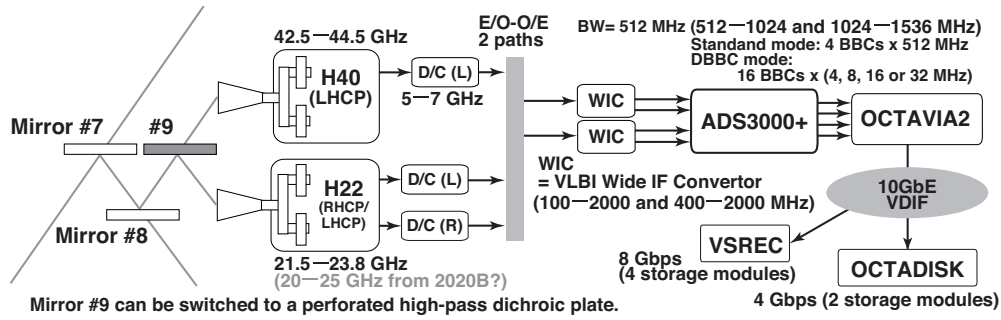
Figure 15: Flow diagram of signals from receiver to recorder for NRO45.

with dual circular polarization. Observations of both single- (LCP) and dual-circular-polarization are available for the EAVN open use. The observable frequency range and the typical receiver noise temperature are shown in Table 5. The total system noise temperatures at K-band is typically 40 K at winter with good weather, > 100 K at winter with bad weather, 150 K at summer with good weather, and > 500 K at summer with bad weather.

For K-band, received RF signals are down-converted into an IF range of $8.0 - 8.8$ GHz, and the IF signals are then mixed down to the base band of $512 - 1024$ MHz, which is the input to the A/D sampler ADS-3000+. The data with the rate of 1024 MHz $\times$ 2 bit are recorded by OCTADISK, and then the digital base-band converter is used to convert the 2 Gbps data into 1 Gbps.
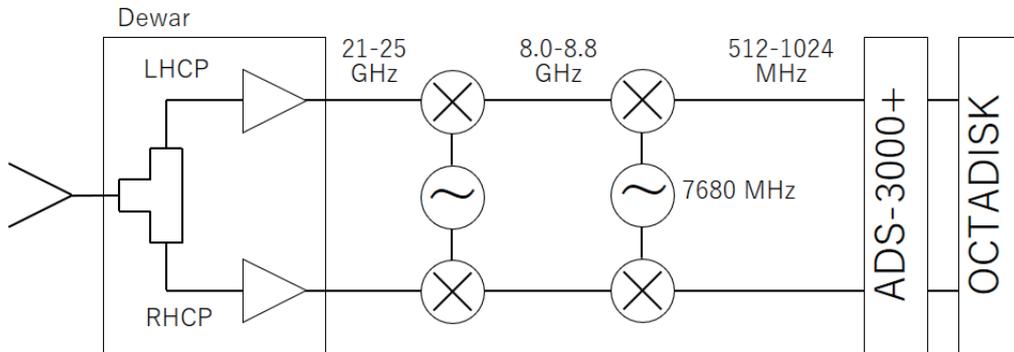
Figure 16: Flow diagram of signals from receiver to recorder for TAK32.

2.3.5 Brief Summary of HIT32 Receiving System

Figure 17 shows a flow diagram of the VLBI receiving system in HIT32. HIT32 covers an observing frequency range of $6.5 - 12.5$ GHz and $21 - 25$ GHz with two cryogenically-cooled receivers, while HIT32 joins in EAVN observations at only C-band in the 2025A semester.

The flow diagram of HIT32 is shown in Figure 17. The C-band receiver is cooled with dual circular polarization. The observable frequency range and the typical receiver noise temperature are shown in Table 5. The total system noise temperatures at C-band is typically 30 K with good weather and $\sim$ 40 K with bad weather.

For C-band, received RF signals are mixed down to the base band of 512 – 1024 MHz, which is the input to the A/D sampler ADS-3000+. The data with the rate of 1024 MHz × 2 bit are recorded by OCTADISK, and then the digital base-band converter is used to convert the 2 Gbps data into 1 Gbps.
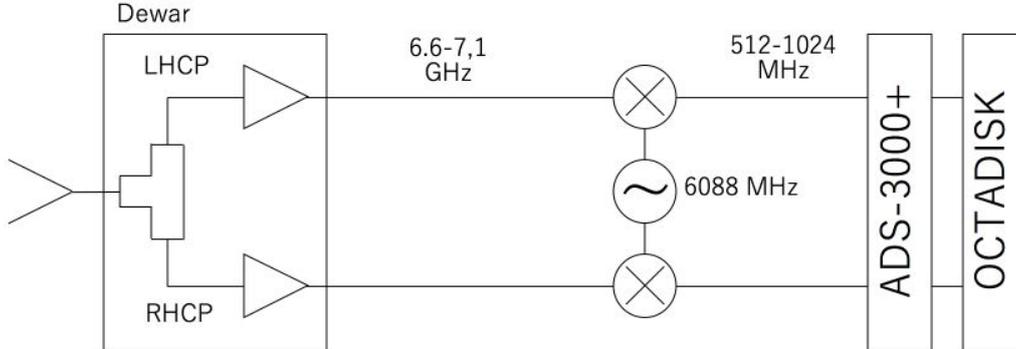
Figure 17: Flow diagram of signals from receiver to recorder for HIT32.

2.3.6 Brief Summary of YAM32 Receiving System

The flow of the VLBI receiving system in YAM32 is the same with that of HIT32. YAM32 covers an observing frequency range of 6 – 9 GHz with a cryogenically-cooled receivers, while YAM32 joins in EAVN observations at only C-band in the 2025A semester.

The C-band receiver is cooled with dual circular polarization. The observable frequency range and the typical receiver noise temperature are shown in Table 5. The total system noise temperatures at C-band is typically 50 K with good weather and ∼ 80 K with bad weather.

For C-band, received RF signals are mixed down to the base band of 512 – 1024 MHz, which is the input to the A/D sampler ADS-3000+. The data with the rate of 1024 MHz × 2 bit are recorded by OCTADISK, and then the digital base-band converter is used to convert the 2 Gbps data into 1 Gbps.

2.3.7 Brief Summary of TMRT65 Receiving System

Figure 18 shows a flow diagram of the VLBI receiving system in TMRT65. TMRT65 has the receivers for 8 frequency bands, L (1.4 GHz), S/X (2.3/8.4 GHz), C (6.7 GHz), X/Ka (8.4/31.0 GHz), Ku (15 GHz), K (22 GHz), and Q (43 GHz). The K- and Q-band receivers are cooled HEMT receivers with dual circular polarizers. The dual-circular-polarization mode is available for open use programs at K- and Q-bands. The observable frequency range and the typical receiver noise temperature are shown in Table 5. The total system noise temperatures at K- and Q-bands are typically 70 and 110 K, respectively. The RF signal is firstly down-converted to IF range of 4 – 12 GHz and it is transferred by optical fibers to the observing room, where the signal is further down-converted to 0 – 1024 MHz (actually in 10 – 512 MHz and 512 – 1024 MHz) at the input of BBCs.
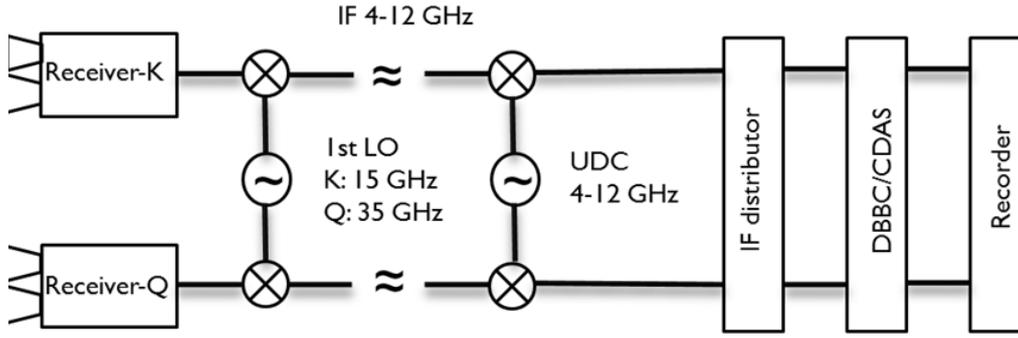
Figure 18: Flow diagram of signals from receiver to recorder for TMRT65.

2.3.8 Brief Summary of SHRT25 Receiving System

The details will be available upon request. Please contact with the EAVN User Support Team if you need further information.

2.3.9 Brief Summary of NSRT26 Receiving System

Figure 19 shows a flow diagram of the VLBI receiving system in NSRT26 at K-band. NSRT26 has the receivers for 5 frequency bands, L (1 – 2 GHz), S/X (2.3/8.4 GHz), C (4 – 8 GHz), K (22 GHz), and Q (43 GHz), while NSRT26 will join in EAVN observations at C-band and K-band in the 2025A semester. The C-band receiver is available for the common-use observations in the 2025A on a shared-risk basis. The C- and K-band receivers are cooled HEMT receivers with dual circular polarizers. Dual-circular-polarization mode is available at the C- and K-bands for open use programs. The observable frequency range and the typical receiver noise temperature are shown in Table 5. The total system noise temperatures at C- and K-bands are typically 50 and 42 K, respectively. The C-band RF signal is down-converted straightly to IF range of 70 – 1024 MHz while the K-band RF signal is down-converted with three stages to IF range of 100 – 600 MHz. The analog-digital conversion and digital filtering of the IF signal for both C- and K-bands are conducted using either the Digital Baseband Converter 2 (DBBC2) system or the Chinese VLBI Data Acquisition System 2 (CDAS2).
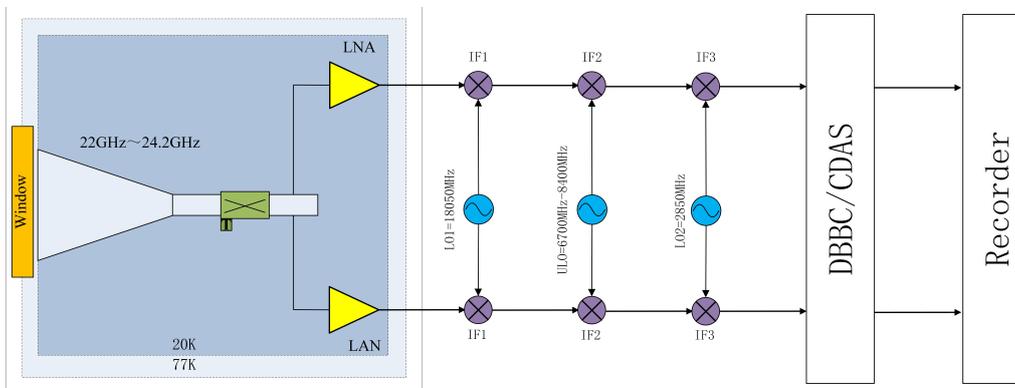
Figure 19: Flow diagram of signals from receiver to recorder for NSRT26 at K-band.

2.3.10 Brief Summary of KMRT40 Receiving System

While the Kunming 40 m telescope will not be available in the 2025A semester due to the problem in the telescope driving system, detailed information is summarized in this section for references.

Figure 20 shows a flow diagram of the VLBI receiving system in KMRT40. KMRT40 has the receivers for 3 frequency bands, S/X (2.2/8.4 GHz), C (4–8 GHz, Lo is tuneable), while KMRT40 joins in EAVN observations at only C-band in the EAVN sessions. The C-band receiver is an HEMT cooled receiver with dual circular polarizations. The observable frequency range and the typical receiver noise temperature are shown in Table 5. The total system noise temperatures at C-band is typically 20 K. The RF signal is down-converted with three stages, and analog-digital conversion and digital filtering of the IF signal is conducted using either the Digital Baseband Converter 2 (DBBC2) system or the Chinese VLBI Data Acquisition System 1 (CDAS1).
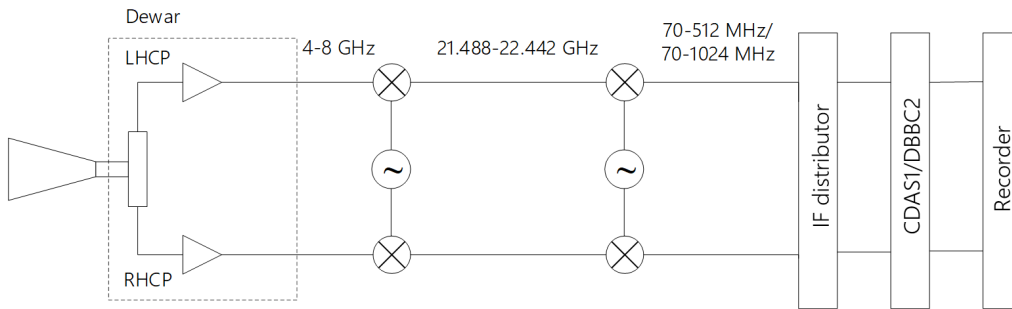
Figure 20: Flow diagram of signals from receiver to recorder for KMRT40.

2.3.11 Brief Summary of KSJ Receiving System

The KSJ antenna has the capability to observe four bands, which are S (2 GHz), X (8 GHz), and simultaneous K/Q (22/43 GHz) bands. Figure 21 shows the layout of quasi-optics and receivers. During the 2025A semester of EAVN observation, only K- and Q- bands are available. For VLBI performance at 22 and 43 GHz, the KSJ telescope was equipped with the same LPF used in the KVN telescope, so the receiver noise temperature was significantly improved, indicating $\sim$ 31 K at 22 GHz and $\sim$ 86 K at 43 GHz. Dual-polarization mode for the KSJ antenna is available from the 2024B semester on a shared-risk basis.

KSJ will not be operational from 2024 November 1 to 2025 February 28 for replacement of the receiver at 22 and 43 GHz.
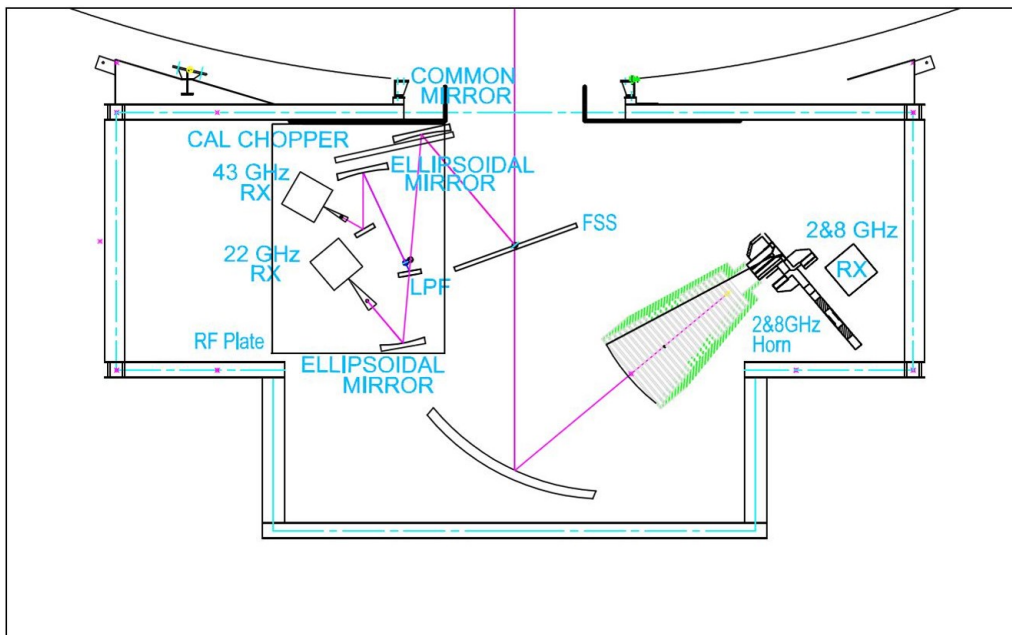
Figure 21: The KSJ quasi-optics and receiving system

2.4 Digital Signal Processing

In VERA system, A/D (analog-digital) samplers convert the analog base band outputs of 0 – 512 MHz × 2 beams to digital form. The A/D converters carry out the digitization of 2-bit sampling with the bandwidth of 512 MHz and the data rate is 2048 Mbps for each beam.

The KVN system provides DFB and OCTAD as backends. The digital filter bank (DFB) is configurable to various modes according to the required number of streams and bandwidths. The DFB enables us to select in frequency domain 16 data streams of 16 MHz bandwidth from 4 streams of 512 MHz bandwidth. The corresponding data rate of the 16 × 16 MHz stream is 1024 Mbps, which corresponds to the maximum input data rate of the Mark5B recorder. Combining more than one stream, the DFB can produce streams with wider bandwidth such as 8 × 32 MHz, 4 × 64 MHz, 2 × 128 MHz, and 1 × 256 MHz. Compared to the DFB, the OCTAD supports a greater number of modes. It enables us to select in the frequency domain a maximum of 16 data streams from 4 streams of 8192 MHz bandwidth. The maximum output rate is 32 Gbps (4 × 8 Gbps) of which the net bandwidth is 8 GHz (4 × 2 GHz bandwidth). There is no restriction on the frequency step and the order of sideband in the OCTAD digital down-converter, unlike the digital filter. In KSJ system, K5 and DBBC3 system are available. The maximum supported data rates of K5 and DBBC3 systems are 1 and 8 Gbps with a 2-bit sampling. With K5 and DBBC3 systems, a simultaneous observing mode of S/X and K/Q bands are supported by the KSJ quasi-optics (Figure 21).

In NRO45 (K-band), TAK32, HIT32, and YAM32 systems, the baseband signal output is 512 – 1024 MHz and the A/D samplers perform 2-bit digitization with four quantization levels. A maximum recording rate of 2048 Mbps is possible with a total bandwidth of 512 MHz. In NRO45 Q-band, the baseband signal output is 1024–1536 MHz.

Since the total data recording rate is limited to 1024 Mbps (see the next section), only part of the sampled data can be recorded onto hard disks. The data rate reduction is done by a digital filter unit (DFU), with which one can flexibly choose number and width of recording frequency bands. Observers can select modes of the DFU listed in the Table 6. In VERA7SIOS mode in the Table 6, two transitions (v=1 & 2) of SiO maser in the Q band can be simultaneously recorded.

When VERA performs the K/Q-band simultaneous observation, GEO1D mode should be selected. Because the common second local oscillator (local frequency ν_{BBCLO}) are used for both K-band and Q-band, the local frequencies in these bands, $\nu_{\text{RF,22 GHz}}$ and $\nu_{\text{RF,43 GHz}}$ shall be linked as follows:

$$\nu_{\text{RF,22 GHz}} = \nu_{\text{1st-LO,22 GHz}} + \nu_{\text{BBCLO}} \tag{2}$$

$$\nu_{\text{RF,43 GHz}} = \nu_{\text{1st-LO,43 GHz}} + \nu_{\text{BBCLO}} \tag{3}$$

Here $\nu_{\text{1st-LO,22 GHz}}$ =16800 MHz and $\nu_{\text{1st-LO,43 GHz}}$ =37500 MHz are fixed. Under this constraint, the K/Q-band simultaneous observation with VERA and NRO45 shall cover the RF frequencies of 21812–22324 MHz (see Section 2.3.3) and 42512–43024 MHz at K-band and Q-band, respectively.

For 1 Gbps dual-polarization recording, either GEO1D (16 MHz × 8 channels × 2 polarizations) or VERA4D (32 MHz × 4 channels × 2 polarizations) must be selected (see Table 7).

Table 6: Digital filter mode for EAVN

Mode Name	Rate (Mbps)	Num. CH[a]	BW/CH[b] (MHz)	CH[c]	Freq. range[d] (MHz)	Side Band[e]	Note for spectral line and VERA dual-beam
GEO1K*	1024	16	16	1	0 - 16	U	
				2	32 - 48	U	
				3	64 - 80	U	
				4	96 - 112	U	
				5	128 - 144	U	
				6	160 - 176	U	
				7	192 - 208	U	
				8	224 - 240	U	
				9	256 - 272	U	Target line (e.g. H_2O)[f]
				10	288 - 304	U	
				11	320 - 336	U	
				12	352 - 368	U	
				13	384 - 400	U	
				14	416 - 432	U	
				15	448 - 464	U	
				16	480 - 496	U	
GEO1S*	1024	16	16	1	112 - 128	L	
				2	128 - 144	U	
				3	144 - 160	L	
				4	160 - 176	U	
				5	176 - 192	L	CH_3OH ($J=5_1$-6_0 A^+)[f]
				6	192 - 208	U	
				7	208 - 224	L	
				8	224 - 240	U	
				9	240 - 256	L	
				10	256 - 272	U	Target line (e.g. H_2O)[f]
				11	272 - 288	L	
				12	288 - 304	U	
				13	304 - 320	L	
				14	320 - 336	U	
				15	336 - 352	L	
				16	352 - 368	U	
VERA7SIOS*	1024	16	16	1	32 - 48	U	
				2	64 - 80	U	
				3	80 - 96	L	SiO ($v=2$, $J=1$-0)
				4	96 - 112	U	
				5	128 - 144	U	
				6	160 - 176	U	
				7	192 - 208	U	
				8	224 - 240	U	
				9	256 - 272	U	
				10	288 - 304	U	
				11	384 - 400	U	SiO ($v=1$ $J=1$-0)
				12	320 - 336	U	
				13	352 - 368	U	
				14	416 - 432	U	
				15	448 - 464	U	
				16	480 - 496	U	

Table 6: Digital filter mode for EAVN — continued.

Mode Name	Rate (Mbps)	Num. CH[a]	BW/CH[b] (MHz)	CH[c]	Freq. range[d] (MHz)	Side Band[e]	Notes for spectral line and VERA dual-beam
VERA4S*	1024	8	32	1	128 - 160	U	
				2	160 - 192	L	
				3	192 - 224	U	
				4	224 - 256	L	
				5	256 - 288	U	
				6	288 - 320	L	
				7	320 - 352	U	
				8	352 - 384	L	
VERA1S*	1024	2	128	1	128 - 256	L	
				2	256 - 384	U	
VERA1**	1024	2	128	1	256 - 384	U	A-Beam
				2	256 - 384	U	B-Beam
VERA7**	1024	16	16	1	256 - 272	U	A-Beam for target line
				2	128 - 144	U	B-Beam (CH 2-16)
				3	144 - 160	L	
				4	160 - 176	U	
				5	176 - 192	L	
				6	192 - 208	U	
				7	208 - 224	L	
				8	224 - 240	U	
				9	240 - 256	L	
				10	256 - 272	U	
				11	272 - 288	L	
				12	288 - 304	U	
				13	304 - 320	L	
				14	320 - 336	U	
				15	336 - 352	L	
				16	352 - 368	U	
VERA7MM**	1024	16	16	1	256 - 272	U	A-Beam for target line
				2	32 - 48	U	B-Beam (CH 2-16)
				3	64 - 80	U	
				4	96 - 112	U	
				5	128 - 144	U	
				6	160 - 176	U	
				7	192 - 208	U	
				8	224 - 240	U	
				9	256 - 272	U	
				10	288 - 304	U	
				11	320 - 336	U	
				12	352 - 368	U	
				13	384 - 400	U	
				14	416 - 432	U	
				15	448 - 464	U	
				16	480 - 496	U	

* All channels are for A-Beam (VERA) and LCP (EAVN).

** Mode for the phase referencing (see section 4.2).

[a] Total number of channels

[b] Bandwidth per channel in MHz

[c] Channel number

[d] Filtered frequency range in the base band (MHz)

[e] Side Band (LSB/USB)

[f] The total local frequency (i.e., RF frequency corresponding to IF = 0 MHz) is 21,971 MHz at K-band for GEO1K and GEO1S, and 6,488 MHz at C-band for GEO1S.

Table 7: Digital filter mode for EAVN dual polarization

Mode Name	Rate (Mbps)	Num. CH[a]	BW/CH[b] (MHz)	CH[c]	Freq. range[d] (MHz)	Side Band[e]	Polarization
GEO1D*	1024	16	16	1	240 - 256	L	RCP
				2	240 - 256	L	LCP
				3	256 - 272	U	RCP
				4	256 - 272	U	LCP
				5	272 - 288	L	RCP
				6	272 - 288	L	LCP
				7	288 - 304	U	RCP
				8	288 - 304	U	LCP
				9	304 - 320	L	RCP
				10	304 - 320	L	LCP
				11	320 - 336	U	RCP
				12	320 - 336	U	LCP
				13	336 - 352	L	RCP
				14	336 - 352	L	LCP
				15	352 - 368	U	RCP
				16	352 - 368	U	LCP
VERA4D*	1024	8	32	1	256 - 288	U	RCP
				2	256 - 288	U	LCP
				3	288 - 320	L	RCP
				4	288 - 320	L	LCP
				5	320 - 352	U	RCP
				6	320 - 352	U	LCP
				7	352 - 384	L	RCP
				8	352 - 384	L	LCP

* GEO1D and VERA4D are also used for K/Q simultaneous mode. In this case, K-band is recorded in
* the channels of odd number (RCP), while Q-band is recorded in the channels of even number (LCP).
[a] Total number of channels
[b] Bandwidth per channel in MHz
[c] Channel number
[d] Filtered frequency range in the base band (MHz)
[e] Side Band (LSB/USB)

2.4.1 Note for DFU copy process

For NRO45, TAK32, HIT32, and YAM32, the recorded data at 2048 Mbps (2 Gbps) are converted to 1024 Mbps (1 Gbps) in the NAOJ Mizusawa correlation center through the digital filter unit (DFU copy). To process the DFU copy, EAVN observations using either NRO45, TAK32, HIT32, and/or YAM32 are required to employ fixed frequency settings (i.e., RF ranges and DFU modes), as listed in Table 8. For the C-band observations (HIT32 and YAM32), frequency settings cannot be changed. For the K-band observations (NRO45 and/or TAK32), fixed DFU mode is required and fixed RF ranges are strongly recommended. If user-specified frequency settings at K-band are required, please consult with the EAVN User Support Team (UST) well in advance. Sample schedule files for these stations are provided on the EAVN website (see Section 5.1).

2.5 Recorders

The EAVN observations are basically limited to record with 1024 Mbps (1 Gbps) data rate. VERA, NRO45, TAK32, HIT32, and YAM32 have OCTADISK. KVN,

Table 8: Frequency settings for the JVN antennas.

Antenna	Band	Mode	DFU	RF (MHz)
HIT32/YAM32	C	C4	VERA4S	6600–6856
		C5	GEO1S	6600–6856
TAK32	K	C4	VERA4S	22099–22355
				22019–22275
		C5	GEO1S	22099–22355
				22048–22304

All settings were already tested by DFU copy process at Mizusawa correlation center. Possible setting with NRO45 will be provided in the future semesters.

TMRT65/SHRT25, NSRT26, and KMRT40 use the Mark5B recording systems. The KSJ use the Mark6 recording system. OCTADISK and Mark5B are hard disk recording systems developed at NAOJ and Haystack observatory, respectively. The total bandwidth is 256 MHz.

2.5.1 Note on the Data Storage Capacity

The data for all EAVN observation are recorded using OCTADISK/Mark5B/Mark6 data recorder depending on the station. EAVN observation data are usually recorded with the data rate of 1 Gbps, while part of observations (e.g., multi-frequency data recording mode at some of EAVN stations) are conducted using higher data sampling rate of greater than or equal to 2 Gbps. This may give rise to shortage of disk space. If it happens, EAVN operation team may ask PI of each EAVN observation to accept revision of the planned observing schedule.

2.6 Correlators

The correlation process is carried out by a VLBI correlator located at KJCC (Korea-Japan Correlation Center) at Daejeon, which has been developed as the KJJVC (Korea-Japan Joint VLBI Correlator) located at KJCC. Hereafter it is tentatively called "Daejeon correlator". Specification of The Daejeon correlator is summarized in Table 9.

The Daejeon correlator can process the data stream of up to 8192 Mbps from maximum 16 antenna stations at once. Currently the raw observed data of KVN, TMRT65/SHRT25, NSRT26, and KMRT40 stations are recorded and playbacked with Mark5B, and those of VERA, NRO45, TAK32, HIT32, and YAM32 are recorded and playbacked with OCTADISK at the data rate of 1024 Mbps. For KaVA, data formats available in 2025A are 16 IFs × 16 MHz ("C5 mode" in The Daejeon correlator terminology), 8 IFs × 32 MHz (C4 mode), and 2 IFs × 128 MHz (C2 mode). For EAVN (including non-KaVA telescopes), available data formats are 16 IFs × 16 MHz (C5 mode) at C- and K-band, and 8 IFs × 32 MHz (C4 mode) at all the C-, K- and Q-bands. Note that the C2 mode is available at only KaVA 8 telescopes because other EAVN telescopes are not equipped with the backend system for the C2 mode. Minimum integration times (time resolution) are 0.2048, 0.8192, and 1.6384 seconds for C2,

Table 9: Specification of The Daejeon correlator[a].

Max. number of antennas	16
correlation mode	C2[b] (128 MHz Bandwidth, 2 stream)
	C4 (32 MHz Bandwidth, 8 stream)
	C5 (16 MHz Bandwidth, 16 stream)
Max. number of corr./input	120 cross + 16 auto
Sub-array	2 case (12+4, 8+8)
Bandwidth	512 MHz
Max. data rate/antenna	2048 Mbps VSI-H (32 parallels, 64 MHz clock)
Max. delay compensation	$\pm$ 36,000 km
Max. fringe tracking	1.075 kHz
FFT work length	16+16 bits fixed point for real, imaginary
Integration time	25.6 msec $\sim$ 10.24 sec
Data output channels	8192 channels
Data output rate	Max. 1.4 GB/sec at 25.6 msec integration time

[a]For more details, see the following website:
https://radio.kasi.re.kr/kjcc/main_kjcc.php
[b]This mode is available for only KaVA.

C4, and C5 modes, respectively, and the number of frequency channels within each IF is 8192 for both modes (i.e. maximum frequency resolution is about 1.95 kHz). By default, the number of frequency channels is reduced to 128 (for continuum) or 512 (for line) via channel integration after correlation. One may put a special request of number of frequency channels to take better frequency resolution. The number of frequency channels can be selected among 512, 1024, 2048, 4096 or 8192. Note that we recommend the maximum frequency channel of 8192 with the C5 mode in the case of CH_3OH maser observations at C-band to achieve sufficient channel and velocity resolution at IF5 (corresponding to 6,664–6,680 MHz. Final correlated data is served as FITS-IDI file.

For the dual-polarization mode at K and Q bands, KJCC currently supports correlation of dual-polarization data up to 12 stations. **Thus, the dual-polarization mode without limitation for the maximum number of telescopes will be open on a shared-risk basis in the 2025A semester.**

2.6.1 Note for the C2 Mode

To obtain the accurate amplitude values across the all IF channels, however, it is better to reduce the number of baseband (or IFs in data handling with AIPS) yielded by the DFU so that the amplitude losses at the edge of each baseband are avoided. This reduction is especially helpful to observe continuum sources, such as active galactic nuclei (AGN). For this purpose, C2 mode, which has 2 IFs $\times$ 128 MHz, is opened for EAVN although the mode can be employed for an observation with only KaVA 8 telescopes.

When using the C2 mode, note the following two matters: (i) There is a moderate amplitude slope in an IF channel mainly at VERA stations, which must be corrected by all the gain calibration procedures in AIPS (AIPS tasks ACCOR, BPASS, and APCAL): (ii) KaVA's observation data is conventionally correlated by the Daejeon

Hardware Correlator. In this case, the scaling factor of 1.3 should be applied to the data to recover the quantization loss [1] [14].

2.7 Calibration

Here we briefly summarize the calibration procedure of the EAVN data. Basically, most of the post-processing calibrations are done by using the AIPS (Astronomical Image Processing System) software package developed by NRAO (National Radio Astronomical Observatory).

2.7.1 Delay and Bandpass Calibration

The time synchronization for each antenna is kept within 0.1 μsec using GPS and high stability frequency standard provided by the hydrogen maser. To correct for clock parameter offsets with better accuracy, bright continuum sources with accurately-known positions should be observed at usually every 60 – 80 minutes during observations. A recommended scan length for calibrators is 5 – 10 minutes. This can be done by the AIPS task FRING. The calibration of frequency characteristic (bandpass calibration) can be also done based on the observation of bright continuum source. This can be done by the AIPS task BPASS.

2.7.2 Gain Calibration

VERA, KVN, NRO45, TAK32, and HIT32 antennas have the chopper wheel of the hot load (black body at the room temperature), and the system noise temperature can be obtained by measuring the ratio of the sky power to the hot load power (so-called R-Sky method). Thus, the measured system noise temperature is a sum of the receiver noise temperature, spillover temperature, and contribution of the atmosphere (i.e. so-called T_{sys}^* corrected for atmospheric opacity). The hot load measurement can be made before/after any scan at all telescopes except TAK32 and HIT32. TAK32 and HIT32 measure the hot-load power at the timing when the telescope operator decides to do the measurement before or after any scan. The sky power is continuously monitored during scans, so that one can trace the variation of the system noise temperature. The system noise temperature value can be converted to SEFD (System Equivalent Flux Density) by dividing by the antenna gain in K/Jy, which is derived from the aperture efficiency and diameter of each antenna. For the correlated data from KJCC, T_{sys}^* data (TY table) and antenna gain information (GC table) are provided with the ANTAB-readable format. KJCC makes complete version of ANTAB-readable file and provide it to PI. User support team supports PIs as appropriate. The TY and GC tables can be loaded by the AIPS task ANTAB, and these tables are converted to the SN table by the AIPS task APCAL.

On the other hand, T_{sys} measurement provided by TMRT65, SHRT25, and NSRT26 contains atmospheric opacity effects, thus the opacity correction should be applied to those data in the course of data reduction.

---

[1]This scaling factor is conventionally applied to the data using the AIPS task APCAL, however this is not applicable if the data is loaded to AIPS using the AIPS task FITLD with DIGICOR = 3.

Alternatively, one can calibrate the visibility amplitude by the template spectrum method, in which auto-correlation spectra of a maser source is used as the flux calibrator. This calibration procedure is made by the AIPS task ACFIT (see AIPS HELP for ACFIT and [5] for more details). For an EAVN observation including TMRT65, NRO45, TAK32, HIT32, NSRT26, and SHRT25, we strongly recommend users to observe a maser source or a compact continuum gain calibrator for every $\leq$ 1 hr. This offers an additional cross-check of the amplitude calibration for TMRT65 and NRO45. YAM32 antenna is not equipped with any system noise temperature measurement system, and hence, it is mandatory to observe a maser source for the gain calibration and absolute flux scaling via the template spectrum method. KMRT40 antenna has a problem with the control program on the system of injecting noise source at each scan during observations, and hence, it is mandatory to observe a maser source for achieving the template spectrum method as well like the situation of YAM32. In particular during elevations lower than 20°, it is recommended to observe these calibrators every 30 min or shorter. Please see Section 3.10 for more details. The DPFU values used in the AIPS task ACFIT are listed in Table 4.

Further correction is made for VLBI observations taken with 2-bit (4-level) sampling, for the systematic effects of non-optimal setting of the quantizer voltage thresholds. This is done by the AIPS task ACCOR. Another correction should be applied to recover the amplitude loss, which are attributed to the combination of two steps of 2-bit quantization in the digital filtering at the backend system and characteristics of Daejeon correlator. This is done by multiplying the scaling factor of 1.3 (the best current estimation) [14] in the AIPS task APCAL (adverbs APARM(1) = 1.3, OPCODE = '', and DOFIT = 1) or SNCOR (adverbs OPCODE = 'MULA', and SNCORPRM(1) = 1.3). Note that this correction should be applied to all EAVN telescopes. The amplitude calibrations with EAVN are accurate to 15% or better at both K- and Q-bands.

For HIT32 at C-band, we recommend to flag the specified frequencies at the beginning of the data reduction: RF 6,600–6,648 MHz due to the IF filtering for anti-alias, and RF 6,712–6,760 MHz due to the Notch-filtering for flagging strong spurious. For example, after the digital filtering with GEO1S mode for HIT32 data, these frequencies correspond to IFs 1–3 and 8–10 in the correlated data in the C5 correlation mode (16 MHz × 16 IFs). This flagging process is done by the AIPS task UVFLG.

2.7.3 Polarization Calibration

EAVN opens a dual-polarization mode at 22 and 43 GHz. The data reduction procedures of polarimectic EAVN data are basically the same as those of other VLBI networks such as VLBA. For polarimetric VLBI data, there are three specific calibration steps, i.e., (1) calibration of the RCP-LCP delays, (2) calibration of polarization leakage terms (D-terms) and (3) absolute electric-vector-polarization angle (EVPA) corrections. For the RCP-LCP delay calibration (that can be performed using the AIPS task RLDLY), one must include a ∼2–3 min scan of a very bright source (usually the source used for fringe-finder and bandpass is fine). For the D-term calibration (that can be performed using the AIPS task LPCAL or GPCAL), one must insert a ∼5–10 min scan of unpolarized or weakly-polarized sources every 1–2 hours covering a sufficient range of parallactic angles. Ideally the calibrators should be sufficiently compact, but moderately-resolved sources may also be used. For the EVPA calibration, one must include some scans of known EVPA sources. Absolute EVPA monitoring of

compact radio sources at 22 or 43 GHz is regularly performed by some single-dish or connected-array facilities such as KVN single dish or VLA. For details, please consult with the support desk of these facilities through the EAVN user support team.

2.7.4 Pointing Correction

The EAVN two large telescopes, TMRT65 and NRO45, will carry out regular antenna pointing scans for every $\leq 1-2$ hr. As for TMRT65, moreover, frequent pointing check is necessary for observations at both K- and Q-bands. The pointing check is done semi-automatically with a continuum back-end system and the quality of pointing check is judged by on-site operators. We strongly recommend to keep at least 3 minutes for the pointing check itself with additional slewing time between target and pointing sources. For example, it is preferable to secure 5-min gap in total for the pointing check toward a pointing source with the angular separation of $\sim 15°$ from the target.

2.8 Geodetic Measurement

2.8.1 Brief Summary of VERA Geodetic Measurement

Geodetic observations are performed as part of the VERA project observations to derive accurate antenna coordinates. The geodetic VLBI observations for VERA are carried out in the S/X-bands and also in the K-band. The S/X-bands are used in the domestic experiments with the Geographical Survey Institute of Japan and the international experiments called IVS-T2. On the other hand, the K-band is used in the VERA internal experiments. We obtain higher accuracy results in the K-band compared with the S/X-bands. The most up-to-date geodetic parameters are derived through geodetic analyses.

Non-linear post seismic movement of Mizusawa after the 2011 off the Pacific coast of Tohoku Earthquake continues. The position and velocity of Mizusawa is continuously monitored by GPS. The coordinates in Table 1 are provisional and will be revised with accumulation of geodetic data by GPS and VLBI.

In order to maintain the antenna position accuracy, the VERA project has three kinds of geodetic observations. The first is participation in JADE (JApanese Dynamic Earth observation by VLBI) organized by GSI (Geographical Survey Institute) and IVS-T2 session in order to link the VERA coordinates to the ITRF2008 (International Terrestrial Reference Frame 2008). Basically Mizusawa station participates in JADE nearly every month. Based on the observations for four years, the three-dimensional positions and velocities of Mizusawa station till 2011 March 9 is determined with accuracies of $7-9$ mm and about 1 mm/yr in ITRF2008 coordinate system. But the uncertainty of several centimeters exists in the position on and after 2011 March 11. The second kind of geodetic observations is monitoring of baseline vectors between VERA stations by internal geodetic VLBI observations. Geodetic positions of VERA antennas relative to Mizusawa antenna are measured from geodetic VLBI observations every two weeks. From polygonal fitting of the six-year geodetic results, the relative positions and velocities are obtained at the precisions of $1-2$ mm and $0.8-1$ mm/yr till 2011 March 10. The third kind is continuous GPS observations at the VERA sites for interpolating VLBI geodetic positions. Daily positions can be determined from 24 hour GPS data. The GPS observations are also used to estimate tropospheric zenith

delay of each VERA site routinely. The time resolution of delay estimates is 5 minutes.

2.8.2 Brief Summary of KVN Geodetic Measurement

The KVN has been participating K band geodetic VLBI observations with the VERA on behalf of KaVA geodesy program since 2011. In addition, the invariant point (IVP) coordinates of the KUS and the KTN telescopes has been measured from the optical survey using GNSS and optical instruments. Please refer [26], for more details. At present, the formal errors of KVN IVP in geodetic VLBI is around 3-5 mm and the difference between VLBI and GNSS is about 2 cm level.

3 Observing Proposal

3.1 Call for Proposals (CfP)

We invite proposals for open-use observations of the EAVN. Please refer to the following EAVN webpage for more details about the array and its performance, and how to prepare and submit a proposal.

<div align="center">https://eavn.kasi.re.kr/</div>

The EAVN open-use call provides opportunities of VLBI observations at 6.7 GHz (C-band), 22 GHz (K-band), and 43 GHz (Q-band) for astronomers in the world. From the 2024B semester, the KPC will be available for each K-, Q-, and simultaneous K/Q-band observations but not for the hybrid mode, on a shared-risk basis. If proposers are not familiar with the EAVN, they are recommended to include at least one collaborator from the EAVN. The contact address for the support is `eavnhelp(at mark)kasi.re.kr`.

Nominal EAVN observations are conducted with single polarization (LCP[2]), while the dual-polarization mode is also available. The data are recorded with the data rate of 1 Gbps for both single- and dual-polarization mode. The data obtained at TAK32, HIT32, and YAM32 are recorded with the data rate of 2 Gbps and reformatted to 1 Gbps data at Mizusawa VLBI Observatory of NAOJ. The total observation time for the EAVN is up to 500 hours, while the available observing time for each EAVN telescope is different between each other, as shown in Table 10.

Special conditions to be considered for EAVN proposal submission are shown below.

3.1.1 Total telescope time and maximum of total request time

Total telescope time to be provided by each telescope/array is as follows. **Note that NRO45 and KMRT40 do not participate in the open-use program in the 2025A semester (Sections 2.2.3 and 2.2.10).**

- Total telescope time for the KaVA is 500 hours in 2025A. Proposers are welcome to request KaVA telescope time without any upper limit. However, for non-KaVA telescopes, the maximum request time per proposal is 50 hours (24 hours for some telescopes). Please refer to the specific conditions for each non-KaVA telescope regarding request time. Please note that proposals for the Large Program will not be accepted for the 2025A semester. Furthermore, it is important to mention that KaVA is a mandatory array for all EAVN observations.

- Sum of total telescope time for TMRT65 is 150 hours in 2025A. Proposers can request for the telescope time of up to 50 hours for TMRT65 for one proposal. Note that proposers cannot request for inclusion of both TMRT65 and SHRT25 in your project. SHRT25 will join EAVN C-band observations in substitution of TMRT65 in case that TMRT65 cannot conduct EAVN observations.

- Total telescope time for NSRT26 is 150 hours. Proposers can request for the telescope time of up to 50 hours for NSRT26 for one proposal.

---

[2]RCP is used for the simultaneous K/Q band mode (see Section 4.5).

Table 10: Available observing time and frequency for each EAVN telescope.

Array/ Telescope	Total time [h]	Max. request time for one proposal [h]	Frequency		
			C-band	K-band	Q-band
KaVA	500	—	●[1]	●	●
Tianma (TMRT65)/	150[2]	50	●	●	●
Sheshan (SHRT25)	—	—	●		
Nanshan (NSRT26)	150	50	●	●	
Takahagi (TAK32)	50	24		●	
Hitachi (HIT32)	50	24	●[4]		
Yamaguchi (YAM32)	50	24	●[4]		
Sejong (KSJ)	50[5]	24		●	●

1: Five telescopes (VERA's 4 telescopes and KUS) out of KaVA's
   8 telescopes join EAVN observations at C-band.
2: Available time of the TMRT65 and SHRT25 antennas is 150h in total
   (not 150h for each).
3: Exactly total time and maximum time for one proposal is depends on
   its national missions, but negotiable.
4: HIT32 and YAM32 are simultaneously involved in EAVN open-use
   observations at C-band. Proposers shall not be able to choose only one of
   either HIT32 or YAM32 for their EAVN observations.
5: The KSJ telescope time is shared between EAVN open-use program (this
   call) and KVN open-use program.

- Total telescope time for TAK32, HIT32, and YAM32 is 50 hours each. Proposers can request for the telescope time of up to 24 hours for each TAK32, HIT32, and YAM32 for one proposal.

- **Total telescope time for KSJ is 50 hours in 2025A. Note that KSJ will not be operational from 2024 November 1 to 2025 February 28 for replacement of the receiver at 22 and 43 GHz.** Proposers can request up to 24 hours of telescope time for a single proposal. This telescope time is shared between the EAVN open-use program (this call) and the KVN open-use program. The process of sharing KSJ's telescope time will be discussed between the Time Allocation Committee of EAVN and KVN based on the results of proposal reviews. Note that KSJ participates in the EAVN open-use program in the 2025A semester with a shared-risk mode for all observing modes.

3.1.2 Term of EAVN observation

- All EAVN observations will be scheduled between 2025 January 16 and 2025 June 15, while possible term of observation for each array/telescope is different between each other, as mentioned below.

- **NRO 45-m, and Kunming 40-m telescopes will not be available in the 2025A semester due to the instrumental problems (Sections 2.2.3 and 2.2.10).**

3.1.3 Possible array configuration

- KaVA is a mandatory array for all EAVN observations.

- At K- and Q-bands, EAVN accepts a request for usage of sub-array configuration (KaVA 8 telescopes and additional telescopes from TMRT65, NSRT26, TAK32, and KSJ for K-band, and KaVA 8 telescopes and additional telescopes from TMRT65, and KSJ for Q-band) as well as EAVN full array configuration with 12 or 10 telescopes at K- or Q-band, respectively. A proposer shall clarify the reason for the choice of sub-array configuration in the proposal.

- HIT32 and YAM32 shall be simultaneously involved in EAVN open-use observations at C-band. Proposers shall not be able to choose only one of either HIT32 or YAM32 for their EAVN observations. Table 11 summarizes possible array configuration for EAVN observations at C-band.

- At C-band, either TMRT65 or SHRT25 will join the EAVN observations. When TMRT65 is not available, SHRT25 will be used in the EAVN observations.

- For the dual-polarization mode at K- and Q-bands, KJCC currently supports correlation of dual-polarization data up to 12 stations. **Thus, the dual-polarization mode without limitation for the maximum number of telescopes will be open on a shared-risk basis.**

Table 11: Possible array configuration at C-band.

Configuration	Telescope				
	KaVA[a]	TMRT65 SHRT25[b]	NSRT26	HIT32[c]	YAM32[c]
1	●				
2	●	○			
3	●		●		
4	●	○	●		
5	●			●	●
6	●	○		●	●
7	●		●	●	●
8	●	○	●	●	●

[a] KaVA includes VERA 4 telescopes and KUS (i.e. total 5 telescopes).
[b] Either TMRT65 or SHRT25 will join EAVN observations.
[c] HIT32 and YAM32 shall be simultaneously involved in EAVN observations.

In summary, non-KaVA telescopes (TMRT65/SHRT25, NSRT26, TAK32, HIT32, YAM32, and KSJ) will participate in EAVN observations together with KaVA according to scientific needs and their availability. Note that proposals submitted to EAVN can be assigned to KaVA according to the decision by the EAVN Time Allocation Committee (TAC). Detailed information on the EAVN call-for-proposal can be found in the following webpage:

https://radio.kasi.re.kr/cfp.php?cate=EAVN

3.2 Proposal Submission

EAVN proposal submission deadline is at

08:00 UT on 1 November, 2024.

The EAVN proposal application form and proposal information are available at the EAVN website:

`https://radio.kasi.re.kr/cfp.php?cate=EAVN`

EAVN proposal shall be submitted via the newly provided online submission system on the following address.

`https://radio.kasi.re.kr/cfp_view.php?id=39&cate=EAVN`

Two PDF documents for a proposal cover sheet (two pages) and a body of proposal including scientific and technical justification including figures and tables (maximum of three pages; minimum font size of 11 points) should be attached on a message. Please send each proposal separately in case of submitting more than one proposal.

Screening results for all submitted proposals will be announced to each PI by early January, 2025. If you have any questions or requests regarding to your proposal, please contact also to `eavnprop(at mark)kasi.re.kr`.

3.3 Special Condition for Selecting Proposals

All submitted proposals for EAVN are reviewed by referees and the EAVN TAC allocates the observing time based on the referee's rating. A proposal submitted for EAVN observations could be allocated as KaVA observations depending on its rating and the decision made by TAC. Proposers thus should specify the necessity of including non-KaVA telescopes in your observations.

3.4 Policy of Recovery Observations

If an open use observation has more than one missing station due to system trouble and/or very severe weather conditions (e.g. strong wind due to a typhoon), the PI can request recovery observations within a year of receiving the correlated data. The EAVN TAC will consider the time allocation of the recovery observations for the next season. This policy is applied to EAVN telescopes except NRO45, KMRT40, and KSJ i.e., KVN, VERA, TMRT65/SHRT25, NSRT26, TAK32, HIT32 and YAM32.

3.5 Policy of One-year-long Proposals

EAVN accepts a proposal which requests observations across two successive semesters (2025A and 2025B semesters). Maximum of total request time for one proposal requesting for one-year-long observation shall be twice the telescope time for that requesting for half-year-long observation, i.e., 100 hours for TMRT65 and NSRT26, 48 hours for TAK32, HIT32, and YAM32, 48 hours for KSJ. No limitation on the total request time

is set for KaVA. Proposers should clarify necessity of time allocation for two successive semesters in the proposal submitted.

Since the 2025A semester, the selection criteria or the successful two-semester-long proposals are revised: Observing time for the second semester (2025B) may be allocated to a two-semester-long proposal by fulfilling one of following two conditions: (a) received the grade 'A' with its score of higher than 8.5. (b) ranked within top 10% of all submitted proposals.

3.6 Observation Mode

EAVN provides opportunities of observations at three observing frequencies, 6.7 GHz (C-band), 22 GHz (K-band), and 43 GHz (Q-band). By default, EAVN observations are conducted with single polarization (LCP[3]) and with the data recording rate of 1 Gbps (total bandwidth of 256 MHz). From the 2024B semester, up to 12 EAVN antennas can be used in the dual-polarization mode. **Thus, the dual-polarization mode is open without any limitation for the maximum number of antennas under the risk-share condition.** Three types of setup of the digital filter ('C2 mode' with 2 IFs × 128 MHz, 'C4 mode' with 8 IFs × 32 MHz, and 'C5 mode' with 16 IFs × 16 MHz) are available, while the C2 mode is not available if your proposal contains requests for usage of non-KaVA stations. The C4 mode is available at all the frequencies, while the C5 mode can be used at both C- and K-bands. EAVN accepts a proposal using the 'Multi-frequency data recording mode' in which KVN records the observation data at more than one frequency, while total number of sessions using this mode might be limited depending on capability of disk storage. **Note that multi-frequency mode and dual-polarization mode cannot be employed simultaneously for the EAVN session in the 2025A semester.**

Available observing mode of EAVN is summarized in Tables 12 and 13.

Table 12: Available observing mode of EAVN.

Frequency	C-band	K-band	Q-band
Telescope	VERA, KUS, TMRT65/SHRT25, NSRT26, HIT32, YAM32 (9 telescopes)	KaVA, KSJ, TMRT65, NSRT26, TAK32 (12 telescopes)	KaVA, KSJ, TMRT65 (10 telescopes)
Backend mode	C4, C5[a]	C2[b], C4, C5	C2[b], C4, C5
Recording rate	1 Gbps[c]	1 Gbps[d]	1 Gbps
Polarization	Left-hand circular polarization (LCP)	LCP[e] or Dual circular polarization	LCP[e] or Dual circular polarization
Correlator	Daejeon Hardware Correlator		

[a] For maser observations, C5 mode is strongly recommended to achieve sufficiently high channel resolution.

[b] C2 mode is available at only KaVA telescopes.

[c] Data obtained at HIT32 and YAM32 are recorded with 2 Gbps and reprocessed to 1 Gbps.

[d] Data obtained at TAK32 are recorded with 2 Gbps and reprocessed to 1 Gbps.

[e] RCP is used for the simultaneous K/Q band mode (see Section 4.5).

---

[3]RCP is used for the simultaneous K/Q band mode (see Section 4.5).

Table 13: Available observing mode for each EAVN telescope.

	Band			Observing mode						
Telescope	C	K	Q	T.I.[a]	F.S.[b]	HB[c]	WFI[d]	K/Q[e,f]	2-pol[f,g]	ToO[h]
KaVA	•[i]	•	•	•	•	•	•	•	•	•
TMRT65	•	•	•	•					•	•
SHRT25	•			•						
NSRT26	•	•		•	•				•(K)	•
TAK32		•		•					•(K)	•
HIT32	•			•	•					•
YAM32	•			•	•					•
KSJ		•	•	•	•			•	•	

[a] Total intensity imaging.
[b] Fast antenna switching. See Section 4.2.
[c] 1-beam hybrid mode. See Section 4.3.
    KPC will be available on a shared-risk basis.
[d] Wide-field imaging with short accumulation period. See Section 4.4.
[e] K/Q-band simultaneous observation mode. See Section 4.5.
[f] K/Q-band multi-frequency mode and dual-polarization mode cannot be employed
    simultaneously for the EAVN session in the 2025A semester.
[g] Dual circular polarization at K- and Q-bands. See Section 4.1
    KSJ will be available on a shared-risk basis.
[h] Target of opportunity. See Section 3.7.
[i] VERA four stations and KUS station.

3.7 Target of Opportunity (ToO) Observations

EAVN accepts ToO proposals. Proposers can request the participation of TMRT65, NSRT26, HIT32, TAK32, and YAM32 as well as KaVA for ToO observations, while these non-KaVA telescopes will join only on a best effort basis. Note that NRO45, KMRT40, and KSJ cannot be included for ToO proposals. Total approved time for ToO proposals is limited to be 100 hours in the 2025A semester.

It is strongly recommended that ToO proposals (especially expected ToO) are submitted during the regular CfP. Unexpected or urgent ToO can be submitted as Director's Discretionary Time (DDT) proposals. ToO proposals must include clear triggering criteria to initiate an observation. ToOs are valid for one year after it is approved. ToO proposals for DDT should follow the same format of regular call and should be sent to `eavnprop(at mark)kasi.re.kr`.

3.8 Angular Resolution and Largest Detectable Angular Scale

The highest angular resolution for EAVN observations is 1.8 mas at C-band for VERA-Ogasawara – NSRT26 baseline, 0.55 mas at K-band for VERA-Ogasawara – NSRT26 baseline, and 0.63 mas at Q-band for VERA-Mizusawa – VERA-Ishigakijima baseline in 2025A. The synthesized beam size strongly depends on UV coverage, and could be larger than the values mentioned above because the baselines projected on UV plane become shorter than the distance between telescopes. The beam size can be calculated approximately by the following formula;

$$\theta \sim 2063 \left(\frac{\lambda}{[\text{cm}]} \right) \left(\frac{B}{[\text{km}]} \right)^{-1} [\text{mas}], \tag{4}$$

where λ and B are observed wavelength in centimeter and the maximum baseline length in kilometer, respectively.

The maximum detectable angular scale for interferometers can be also expressed by equation (4), where the baseline length B is replaced with the shortest one among the array.

Because of the relatively short baselines provided by KVN ($\sim$130 km between KYS and KPC), KaVA is able to detect an extended structure up to 23 mas and 11 mas for the K- and Q-bands, respectively. When the KSJ antenna is included in the EAVN observations, the shortest baseline length becomes 120 km between the KYS and KSJ stations. In the case of C-band, the first, second, and third shortest baseline formed by KUS – YAM32, VERA-Mizusawa – HIT32 and VERA-Iriki – YAM32 is similar to be $\sim$260 km, $\sim$270 km and $\sim$290 km, yielding 36, 34 and 32 mas in C-band, respectively.

3.9 Sensitivity

When a target source is observed, a noise level σ_{bl} for each baseline in the single-polarization can be expressed as

$$\sigma_{\mathrm{bl}} = \frac{2k}{\eta} \frac{\sqrt{T_{\mathrm{sys},1} T_{\mathrm{sys},2}}}{\sqrt{A_{e,1} A_{e,2}} \sqrt{2B\tau}} = \frac{1}{\eta} \frac{\sqrt{SEFD_1 SEFD_2}}{\sqrt{2B\tau}}, \tag{5}$$

where k is Boltzmann constant, η is quantization efficiency (~ 0.88), T_{sys} is system noise temperature, $SEFD$ is system equivalent flux density, A_e is antenna effective aperture area ($A_e = \pi \eta_A D^2/4$ in which η_A and D are the aperture efficiency and antenna diameter, respectively), B is the bandwidth, and τ is on-source integration time. Note that for an integration time beyond 3 minutes (in the K-band), the noise level expected by equation (5) cannot be attained because of the coherence loss due to the atmospheric fluctuation. Thus, for finding fringe within a coherence time, the integration time τ cannot be longer than 3 minutes. For VLBI observations, signal-to-noise ratio (S/N) of at least 5 and usually 7 is generally required for finding fringes.

A resultant image noise level σ_{im} can be expressed as

$$\sigma_{\mathrm{im}} = \frac{1}{\sqrt{\Sigma \sigma_{\mathrm{bl}}^{-2}}}. \tag{6}$$

If the array consists of identical antennas, an image noise levels can be expressed as

$$\sigma_{\mathrm{im}} = \frac{2k}{\eta} \frac{T_{\mathrm{sys}}}{A_e \sqrt{N(N-1)B\tau}} = \frac{1}{\eta} \frac{SEFD}{\sqrt{N(N-1)B\tau}}, \tag{7}$$

where N is the number of antennas.

Using the typical parameters shown in Tables 14–16, baseline sensitivities of KVN, VERA, and EAVN antennas in the single-polarization mode are calculated as listed in Tables 14–16. Based on these baseline sensitivity values, image sensitivities for all possible array configurations of EAVN in the single-polarization mode are also provided in Tables 17–18.

Figures 22 and 23 show the system noise temperature at VERA in K/Q-bands, VERA-Ogasawara in C-band, and KUS in K/Q-bands, respectively. For VERA, receiver noise temperatures are also plotted.

Note that the receiver temperature of VERA includes the temperature increase due to the feedome loss and the spill-over effect. In Mizusawa, typical system temperature in the K-band is $T_{\mathrm{sys}} = 150$ K in fine weather of winter season, but sometimes rises above $T_{\mathrm{sys}} = 300$ K in summer season. The system temperature at Iriki station shows a similar tendency to that in Mizusawa. In Ogasawara and Ishigakijima, typical system temperature is similar to that for summer in Mizusawa site, with typical optical depth of $\tau_0 = 0.2 \sim 0.3$. The typical system temperature in the Q-band in Mizusawa is $T_{\mathrm{sys}} = 250$ K in fine weather of winter season, and $T_{\mathrm{sys}} = 300 - 400$ K in summer season. The typical system temperature in Ogasawara and Ishigakijima in the Q-band is larger than that in Mizusawa.

On the other hand, system noise temperature in C-band is stable around 100–150 K at all the VERA stations through all the season with typical zenith optical depth of $\tau_0 = 0.03 \sim 0.04$, although it sometimes show larger values due to extremely bad weather condition.

The typical system temperature in the K-band at all KVN stations is around 100 K in winter season. In summer season, it increases up to ~ 300 K. In the Q-band, the typical system temperature is around 150 K in winter season and 250 K in summer season at KYS and KTN. The system temperature of KUS in the Q-band is about 40 K lower than the other two KVN stations. This is mainly due to the difference in receiver noise temperature (see Table 5).

In the dual-polarization mode, the baseline sensitivity to each polarization will be degraded by a factor of $\sqrt{1/2}$ since the total recording rate is fixed to 1 Gbps and the bandwidth for each polarization becomes a half of that in the single polarization mode.

Table 14: Performance of EAVN at K-band

	Antenna performance			Baseline sensitivity					
	T_{sys} [K]	η_{A}	SEFD [Jy]	KVN	VERA	TMRT65	NSRT26	TAK32	KSJ
KVN[a]	100	0.71	1122	5.1	7.1	1.5	2.9	3.3	4.9
VERA	120	0.50	2108	–	9.7	2.1	4.0	4.5	6.8
TMRT65	60	0.50	100	–	–	–	0.9	1.0	1.5
NSRT26	42	0.60	364	–	–	–	–	1.9	2.8
TAK32	40	0.30	458	–	–	–	–	–	3.2
KSJ	100	0.70	1037	–	–	–	–	–	–

Note: The 1σ baseline sensitivity values for the single-polarization are listed in unit of mJy, which assume an integration time of 120 seconds and a bandwidth of 256 MHz for the calculation. In the case of narrower bandwidth of 15.625 kHz (i.e., velocity resolution of 0.21 km s^{-1} for maser emission), sensitivities can be calculated by multiplying a factor of $\sqrt{256 \text{ MHz}/15.625 \text{ kHz}} = 128$.
[a] The averaged value over the four telescopes of the KVN, including Pyeongchang.
For more information, see the KVN status report[2].

3.10 Calibrator Information

The NRAO VLBA calibrator survey is very useful to search for a continuum source which can be used as a reference source to carry out the delay, bandpass, and phase calibrations. The source list of this calibrator survey can be found at the following VLBA homepage:

Table 15: Performance of EAVN at Q-band

	Antenna performance			Baseline sensitivity			
	T_{sys} [K]	η_{A}	SEFD [Jy]	KVN	VERA	TMRT65	KSJ
KVN[a]	150	0.69	1732	7.9	12.6	2.1	7.8
VERA	250	0.50	4393	–	20.1	3.4	12.3
TMRT65	66	0.45	122	–	–	–	2.1
KSJ	150	0.66	1650	–	–	–	—

Note: The 1σ baseline sensitivity values for the single-polarization are listed in unit of mJy, which assume an integration time of 120 seconds and a bandwidth of 256 MHz for the calculation. In the case of narrower bandwidth of 15.625 kHz (i.e., velocity resolution of 0.11 km s^{-1} for maser emission), sensitivities can be calculated by multiplying a factor of $\sqrt{256\ \mathrm{MHz}/15.625\ \mathrm{kHz}} = 128$.
[a] The averaged value over the four telescopes of the KVN, including Pyeongchang. For more information, see the KVN status report[2].

Table 16: Performance of EAVN at C-band

	Antenna performance			Baseline sensitivity					
	T_{sys} [K]	η_{A}	SEFD [Jy]	VERA	TMRT65	SHRT25	NSRT26	HIT32	YAM32
KUS	330	0.62	4241	13.9	2.2	12.5	7.1	3.8	5.0
VERA	130	0.53	2155	9.9	1.6	8.9	5.1	2.7	3.6
TMRT65	30	0.45	55	–	–	–	0.8	0.4	0.6
SHRT25	130	0.42	1740	–	–	–	4.6	2.4	3.2
NSRT26	55	0.50	572	–	–	–	–	1.4	1.9
HIT32	30	0.65	158	–	–	–	–	–	1.0
YAM32	50	0.60	286	–	–	–	–	–	–

Note: The 1σ baseline sensitivity values for the single-polarization are listed in unit of mJy, which assume an integration time of 120 seconds and a bandwidth of 256 MHz for the calculation. In the case of narrower bandwidth of 1.953125 kHz (i.e., velocity resolution of 0.088 km s^{-1} for maser emission), sensitivities can be calculated by multiplying a factor of $\sqrt{256\ \mathrm{MHz}/1.953125\ \mathrm{kHz}} \sim 362$.

```
http://www.vlba.nrao.edu/astro/calib/index.shtml
https://obs.vlba.nrao.edu/cst/
```

For delay calibrations and bandpass calibrations, calibrators with 1 Jy or brighter are strongly recommended as listed in the VLBA fringe finder survey:

```
http://www.vlba.nrao.edu/astro/fringe_finder_survey/ffs.html
https://science.nrao.edu/facilities/vlba/publications/memos/test/ffs
```

Interval of observing calibrator scans must be shorter than 1 hour to track the delay and delay rate in the correlation process.

If you request the participation of the YAM32 and/or KMRT40 and/or NSRT26 antennas for observations in C-band, it is mandatory to do gain calibration and absolute flux scaling by the template spectrum method. In this method, a strong and compact CH_3OH maser source which locates within 15° from the target source should be observed with an interval of 1 hr or shorter. In particular during elevations lower than 20°, it is recommended to observe these calibrators every 30 min or shorter. Even

Table 17: Image sensitivity of EAVN at K- and Q-bands.

Array	N_{ant}	N_{bl}	K-band	Q-band
KaVA	8	28	199	348
KaVA+TMRT65	9	36	80	119
KaVA+NSRT26	9	36	128	–
KaVA+TAK32	9	36	137	–
KaVA+KSJ	9	36	163	279
KaVA+TMRT65+NSRT26	10	45	61	–
KaVA+TMRT65+TAK32	10	45	64	–
KaVA+TMRT65+KSJ	10	45	71	106
KaVA+NSRT26+TAK32	10	45	97	–
KaVA+NSRT26+KSJ	10	45	111	–
KaVA+TAK32+KSJ	10	45	118	–
KaVA+TMRT65+NSRT26+TAK32	11	55	51	–
KaVA+TMRT65+NSRT26+KSJ	11	55	56	–
KaVA+TMRT65+TAK32+KSJ	11	55	58	–
KaVA+NSRT26+TAK32+KSJ	11	55	87	–
KaVA+TMRT65+NSRT26+TAK32+KSJ	12	66	48	–

Note: N_{ant} and N_{bl} are the numbers of telescopes and baselines for each array, respectively. The 1σ image sensitivity values in the single-polarization mode are listed in unit of μJy, which assume an integration time of 4 hours and a total bandwidth of 256 MHz for the calculation. In the case of narrower bandwidth of 15.625 kHz for maser emission in K/Q-bands, sensitivities can be calculated by multiplying a factor of 128.

if YAM32 and/or KMRT40 and/or NSRT26 antennas are not included in the observations, it is recommended to observe the strong and compact CH_3OH maser source with the same interval as the cross-check for the gain curve and absolute flux scaling of the TMRT65 antenna as well. The 6.7 GHz CH_3OH maser sources close to your target sources can be found in the following catalog papers (NOTE: in the template spectrum method for the TMRT65 in C-band, it is NOT recommended that the 6.7 GHz CH_3OH maser sources 009.621+0.196, 133.94+1.04 (W3(OH) / W3-IRS5), and 351.417+0.645 & 351.417+0.646 (NGC6334F) are selected because these sources are too strong for the TMRT65 to guarantee an accuracy of the absolute flux scaling.):

Methanol MultiBeam (MMB) Survey:

$20° \leq l \leq 60°$: https://academic.oup.com/mnras/article/450/4/4109/1747594
$6° \leq l \leq 20°$: https://academic.oup.com/mnras/article/409/3/913/1094145
$345° \leq l \leq 6°$: https://academic.oup.com/mnras/article/404/2/1029/968927
$330° \leq l \leq 345°$: https://academic.oup.com/mnras/article/417/3/1964/1090874
$186° \leq l \leq 330°$: https://academic.oup.com/mnras/article/420/4/3108/972699

Ibaraki 6.7 GHz class II methanol maser database (iMet):

http://vlbi.sci.ibaraki.ac.jp/iMet/

Other catalog for sources in more northern hemisphere:

https://www.aanda.org/articles/aa/abs/2009/44/aa12135-09/aa12135-09.html

Table 18: Image sensitivity of EAVN at C-band.

Array	N_{ant}	N_{bl}	C-band
KaVA	5	10	450
KaVA+TMRT65	6	15	94
KaVA+NSRT26	6	15	255
KaVA+TMRT65+NSRT26	7	21	68
KaVA+HIT32+YAM32	7	21	89
KaVA+TMRT65+HIT32+YAM32	8	28	37
KaVA+NSRT26+HIT32+YAM32	8	28	73
KaVA+TMRT65+NSRT26+HIT32+YAM32	9	36	34
In the case that SHRT25 joins (when TMRT65 is not available)			
KaVA+SHRT25	6	15	346
KaVA+SHRT25+NSRT26	7	21	215
KaVA+SHRT25+HIT32+YAM32	8	28	83
KaVA+SHRT25+NSRT26+HIT32+YAM32	9	36	69

Note: N_{ant} and N_{bl} are the numbers of telescopes and baselines for each array, respectively. The 1σ image sensitivity values in the single-polarization mode are listed in unit of μJy, which assume an integration time of 4 hours and a total bandwidth of 256 MHz for the calculation. In the case of narrower bandwidth of 1.953 kHz for maser emission in C-band, sensitivities can be calculated by multiplying a factor of 362.

For dual-polarization analysis, one should include calibrators for (1) calibration of the RCP-LCP delays, (2) calibration of polarization leakage terms (D-terms) and (3) EVPA corrections. See also Section 2.7.3 for more detail.

3.11   Data Archive

The users who proposed the observations will have an exclusive access the data for 18 months after the correlation. After that period, all data for EAVN open-use observations will be released as archive data. Thereafter, archived data will be available to any user upon request. This policy is applied to each observation, even if the proposed observation is comprised of multi-epoch observations in this season.
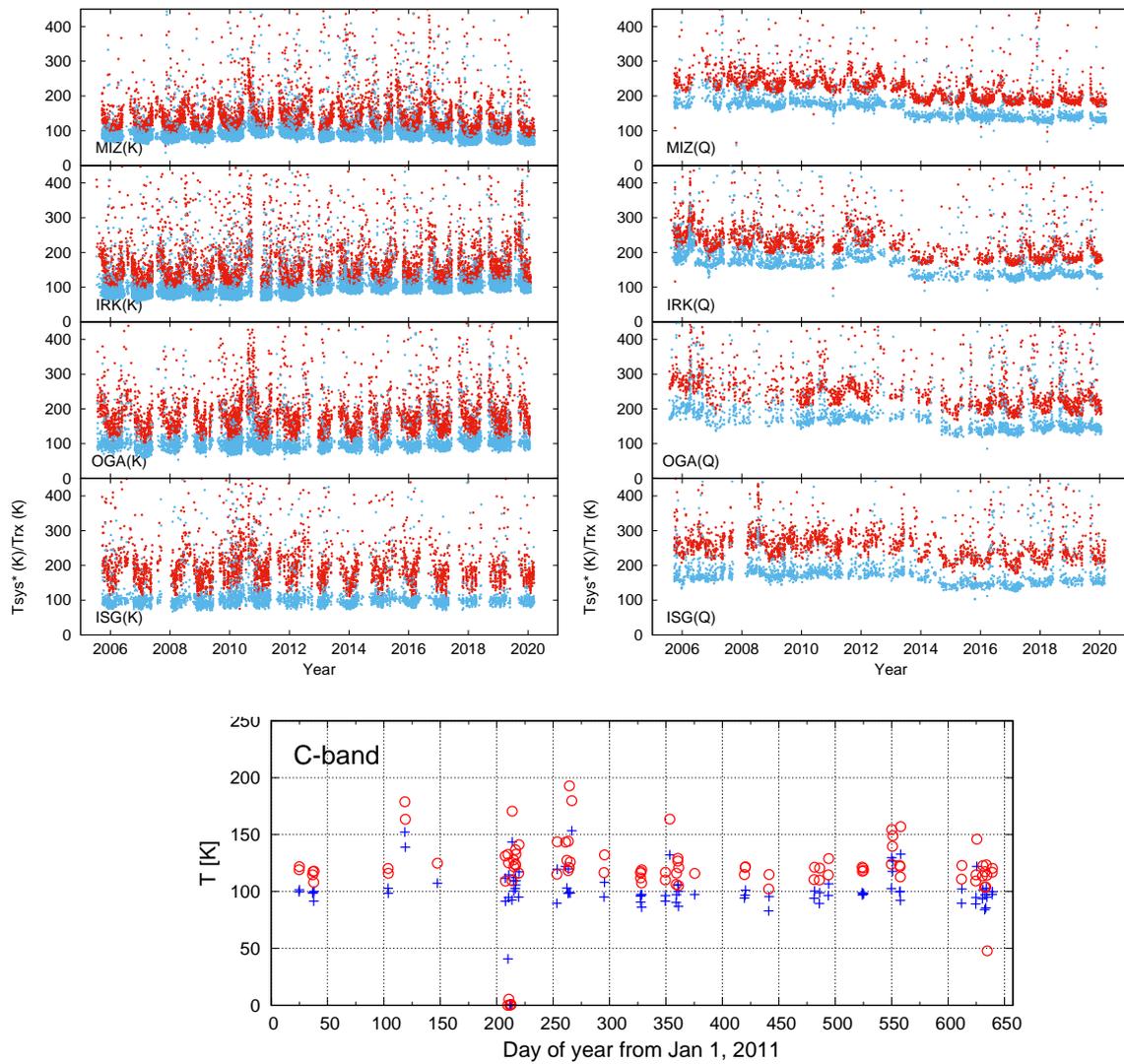
Figure 22: The receiver noise temperature (*blue*) and the system noise temperature (*red*) at the zenith for the VERA antennas at K-band (top-left), Q-band (top-right), and at C-band in Ogasawara station (bottom).
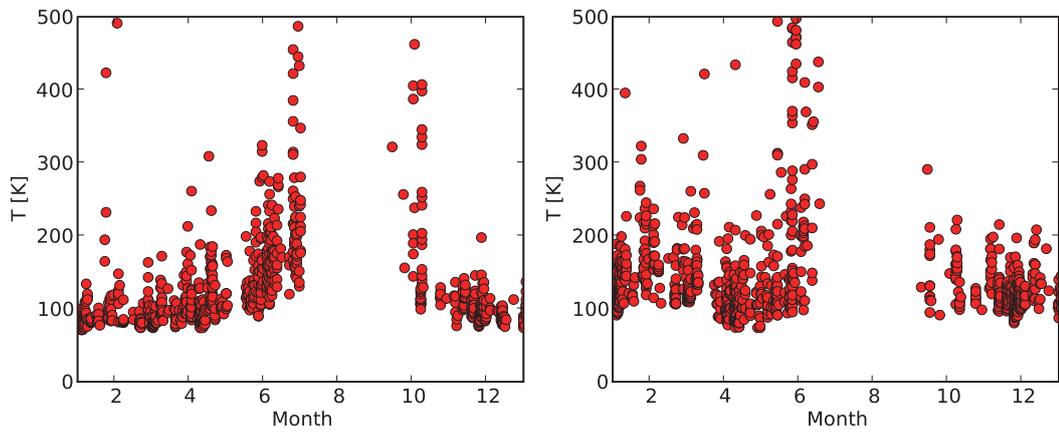
Figure 23: The zenith system noise temperature (*red filled circles*) at K-band (left) and Q-band (right) in KVN-Ulsan station.

4 Notes for Special Modes

In this section, we summarize additional information about special observing/data analysis modes.

4.1 Dual Circular Polarization

The dual-circular-polarization mode is available at the K- and Q-band without any limitation for the maximum number of antennas from the EAVN open use 2025A on a risk-shared basis. The EAVN performance evaluation team (PET) is now verifying polarimetry observation data by comparing the newly correlated data from KJCC and DiFX. **Note that multi-frequency mode and dual-polarization mode cannot be employed simultaneously for the EAVN session in the 2025A semester.** Further details will be available upon request through the EAVN user support team.

4.2 Phase-referencing and Astrometry

EAVN is capable of phase-referencing observations to image weak target sources, which cannot be detected within coherent time, and to conduct absolute astrometry measurements. Note that astrometry capability has been confirmed for K-band observations with KaVA 7 telescopes **(except for the new KPC telescope)**. Although we do not prevent EAVN proposers from submitting proposals with the phase-referencing mode at Q-band and/or with the mode using non-KaVA telescopes within the maximum driving speed of each antenna shown in Table 3, the data quality is not guaranteed. From the semester 2021A, we opened the fast-switching (not astrometry mode) mode in C-band as well. In 2025A, the following antenna combination among KaVA+NSRT26+HIT32+YAM32 is available (see the notification in sub-section 4.2.1).

4.2.1 Fast Switching

Fast switching observation with EAVN is recommended for phase referencing (and astrometry) since the verification of the fast switching with EAVN has been finished, **except for TMRT65, NRO45, TAK32, and KPC telescopes**. In this mode, the antenna nods between phase calibrator (reference) and target source. With this mode, we can detect and image weak sources, which can not be imaged directly by fringe fitting. Regarding antenna switching cycle, users can refer to Table 19.

4.2.2 Notification for Switching Cycle in C-band

In the fast-switching in C-band, we recommend typical time of each switching cycle of 5–6 min, which was observationally verified successful phase-referencing imaging without serious issues and a few milliarcsecond accuracies of absolute position measurements. When you decide the switching cycle, it is necessary to take into account the slewing time of HIT32 that has the slowest driving speed of $0.2°$ sec^{-1}. We thus present a simulated result of antenna slewing time of HIT32. Figure 24 plots the relationship between the slewing time in one way between target and reference continuum

Table 19: Phase-Referencing Cycle Times (min).*

	Typical weather		Bad weather		Good weather	
	$(C_n{}^\dagger = 2\times10^7 \text{ m}^{-1/3})$		$(C_n{}^\dagger = 4\times10^7 \text{ m}^{-1/3})$		$(C_n{}^\dagger = 1\times10^7 \text{ m}^{-1/3})$	
	Frequency (GHz)		Frequency (GHz)		Frequency (GHz)	
EL (deg)	22	$(43)^\ddagger$	22	$(43)^\ddagger$	22	$(43)^\ddagger$
5	0.3	0.2	0.2	0.1	0.8	0.4
10	0.5	0.3	0.2	0.1	0.8	0.6
15	0.7	0.3	0.3	0.1	1.5	0.7
20	0.8	0.4	0.3	0.2	1.8	0.9
25	0.9	0.4	0.4	0.2	2.0	1.0
30	1.0	0.5	0.4	0.2	2.8	1.1
40	1.1	0.5	0.5	0.2	5.8	1.3
50	1.3	0.6	0.6	0.3	9.9	1.5
60	1.8	0.7	0.6	0.3	10.0	2.2
70	2.3	0.7	0.6	0.3	10.0	2.9
80	2.6	0.7	0.6	0.3	10.0	3.3

* Referring to Ulvestad, J., Phase-Referencing Cycle Times, VLBA Scientific Memo 20 (1999).
† C_n is strength of the tropospheric turbulence.
‡ Currently, Q-band phase-referencing mode is under evaluation.
Column 1 shows antenna elevation angles. Columns 2-3 indicate phase-referencing cycles at 22 and 43 GHz, respectively, under typical weather condition. The phase-referencing cycle is defined as the time between the midpoints of the two calibrator observations before and after the target observation. Columns 4-5 are the same as Columns 2-3, but with bad weather condition (similar to some summer days). Columns 6-7 are the same as Columns 2-3, but with good weather condition (similar to some winter nights).

sources as a function of elevation angles for the target–calibrator separation angles (S.A.) of 1 and 2 deg. From Figure 24, it is strongly recommended to schedule the fast-switching observations with elevation angles lower than 80 and 70 deg in the case of S.A. of 1 and 2 deg, respectively. Finally, proposers are required to specify each on-source time for target and reference continuum sources in one switching cycle at C-band in scientific or technical justification in the proposal.

4.2.3 Separation Angle between Target and Phase Reference

It is strongly recommended to observe a pair sources with a small separation angle (e.g., less than 1 degree) at high elevation for precise astrometry. For instance, it is demonstrated that the dynamic range of the phase-referenced image is inversely proportional to the sine of the calibrator-to-target separation as

$$D_1 = \left(\frac{\sqrt{\Delta t}}{K\nu}\right) (\sin\theta_{\text{sep}})^{-1}, \tag{8}$$

where Δt is the on-source observing time, ν, the observing frequency, θ_{sep}, the separation angle between the target and calibrator, and K, a constant to be determined [15].

4.2.4 Tropospheric Calibration with GPS or JMA or Geodetic Blocks

Generally, residual of atmospheric zenith delay dominates cm-wave VLBI positional accuracy. Atmospheric (tropospheric) calibration for EAVN has three options (see
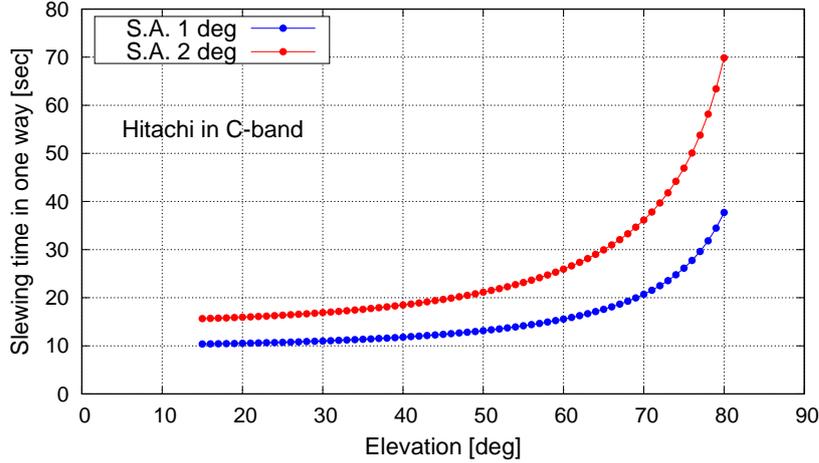
Figure 24: Simulated result of antenna slewing time of HIT32 at C-band in one way between target and reference continuum sources. This simulation shows a dependence on elevation, and a difference in the case of the separation angle of 1 deg (*blue filled circles*) and 2 deg (*red filled circles*).

Table 20), which are (1) GPS, (2) Japan Meteorological Agency (JMA) meso-scale analysis data (Hobiger et al. 2008; JMA Numerical Weather Prediction[4]), and (3) Geodetic blocks[5]. An error of tropospheric zenith delay ($c\Delta\tau_{\mathrm{trop}}$) can be suppressed within ~2 cm with GPS, JMA and Geodetic blocks [11, 16].

Table 20: Tropospheric calibration for each EAVN telescope*.

Telescope	Method		
	GPS	JMA	Geodetic blocks
VERA	●	●	●
KVN	△	●	●
TMRT65	△	●	●
NSRT26	△	×	●

* TMRT65 = Tianma 65m. NSRT26 = Nanshan 26m. ● = Available. △ = These GPS receivers should be evaluated for the usage of astronomical (i.e., astrometry) purpose. × = Not available.

4.2.5 Astrometric Accuracy

We have verified astrometric accuracies of KaVA and EAVN based on (1) a Galactic line source and (2) QSO pair observations (see Figures 25 and 26, and Tables 21 and 22). Single-epoch (relative) astrometric error consists of (1) thermal and (2) systematic errors as shown below [22]:

$$\Delta\theta_{\mathrm{therm}} \approx 31 \left(\frac{22}{\nu\,[\mathrm{GHz}]}\right)\left(\frac{2{,}300}{B_{\mathrm{max}}\,[\mathrm{km}]}\right)\left(\frac{20}{\mathrm{S/N}}\right)[\mu\mathrm{as}] \qquad (9)$$

---

[4]https://www.jma.go.jp/jma/jma-eng/jma-center/nwp/nwp-top.htm
[5]http://bessel.vlbi-astrometry.org/tech

and

$$\Delta s_{\rm rel} \approx 31 \left(\frac{{\rm c}\Delta\tau \ [{\rm cm}]}{2} \right) \left(\frac{2,300}{B_{\rm max} \ [{\rm km}]} \right) \left(\frac{\theta_{\rm sep} \ [{\rm deg}]}{1} \right) \ [\mu{\rm as}] \qquad (10)$$

where ν is the observing frequency, $B_{\rm max}$, the longest baseline length, S/N, signal-to-noise ratio of a phase-referenced image, c$\Delta\tau$, the speed of light multiplied by delay residual, and $\theta_{\rm sep}$, separation angle between the target and a calibrator (a phase reference).
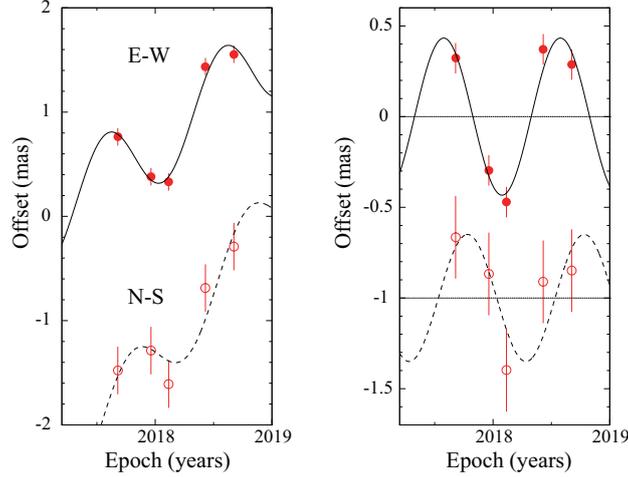
Figure 25: Results of parallax and proper-motion fitting. Plotted are position offset of maser spot (W3(OH) at $V_{\rm LSR} = -47.5$ km s^{-1}) with respect to the background QSO J0244+6228 (with a separation angle of 2.2 degrees) toward the east (R.A.cosσ) and north (σ) as a function of time. For clarity, the north direction data is plotted offset from the east direction data. (*Left*) The best-fit models in the east and north directions are shown as continuous and dashed curves, respectively. (*Right*) Same as the Left, but with proper motions removed.

Table 21: Parallax results for W3(OH)*.

Array	Frequency GHz	Source	$V_{\rm LSR}$ km s^{-1}	Parallax (mas)	$\sigma_{\alpha\cos\delta}$* (mas)	σ_δ* (mas)	Ref.
KaVA	22	W3OH	-47.5	0.460±0.035	0.052	0.256	
VLBA	22	W3OH	-51.5∼-48.2	0.489±0.017	∼0.050	∼0.050	(1)

*Positional errors in right ascension and declination were adjusted so that the reduced chi-square becomes unity. Columns 1-2 represent array and observing frequency. Columns 3-4 show source name and LSR velocity of the maser spot, used for the parallax fit. Column 5 displays the parallax result in milli-arcseconds (mas). Columns 6-7 represent the (systematic) positional errors in right ascension and declination, respectively.
Ref. (1) Hachisuka et al. (2006).

4.2.6   Baseline Length

The longest baseline length is related to astrometric accuracy as shown in Equations (9) and (10). Baseline lengths for EAVN astrometry are compiled in Table 23.
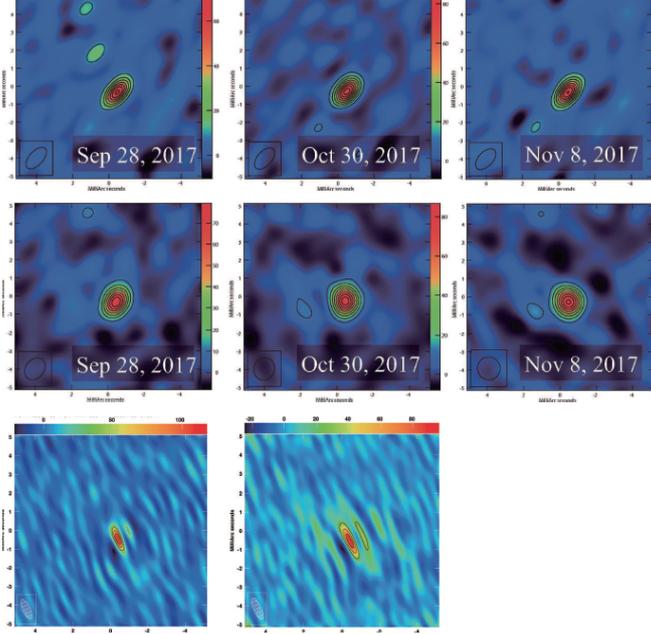
Figure 26: **(Top row)** Phase-referenced images of 0556+238 with VERA, relative to the phase reference 0601+245. The dates of the observations are Sep 28, Oct 30 and Nov 8 in 2017 from left to right. **(Middle row)** Same as the top row, but for KaVA data used. **(Bottom row)** Same as the top row, but for EAVN data used. Observation dates are Mar 27 and May 24 in 2019 from left to right.

Table 22: Results of position repeatability for 0556+238.

	VERA		KaVA		EAVN	
Observation date	R.A.	Decl.	R.A.	Decl.	R.A.	Decl.
	(μas)	(μas)	(μas)	(μas)	(μas)	(μas)
2017/Sep/28	-465 ± 15	-332 ± 16	-451 ± 15	-331 ± 15	$-$	$-$
2017Oct/30	-494 ± 11	-283 ± 12	-462 ± 16	-258 ± 18	$-$	$-$
2017/Nov/8	-505 ± 09	-318 ± 10	-480 ± 13	-287 ± 14	$-$	$-$
2019/Mar/27	-463 ± 21	-343 ± 24	-464 ± 14	-336 ± 17	-407 ± 11	-455 ± 21
2019/May/24	-576 ± 85	-479 ± 150	-592 ± 29	-434 ± 35	-411 ± 24	-524 ± 44
Unweighted mean	$-500\pm21^*$	$-351\pm35^*$	$-490\pm26^*$	$-330\pm30^*$	$-409\pm2^*$	$-490\pm35^*$

Column 1 shows the date of observation. Columns 2-3 display image positions of 0556+238 relative to 0601+245 in right ascension and declination, respectively. Note that the image positions were measured for VERA data. The errors of the positions represent the thermal error. Columns 4-5 are the same as the Columns 2-3, but for KaVA data used. Columns 6-7 are the same as the Columns 2-3, but for EAVN data used.
*The standard error.

Table 23: Baseline lengths for EAVN astrometry.*

	MIZ	IRK	OGA	ISG	KYS	KUS	KTN	KPC	TM65	NS26	SH25	HIT32	YAM32	KM40
MIZ														
IRK	1,300													
OGA	1,300	1,300												
ISG	2,300	1,000	1,800											
KYS	1,200	700	1,800	1,500										
KUS	1,100	400	1,500	1,300	300									
KTN	1,500	400	1,700	1,000	500	400								
KPC	1,100	700	1,700	1,500	100	200	500							
TM65	2,000	900	2,100	800	900	900	600	1,000						
NS26	4,500	4,000	5,200	4,000	3,400	3,700	3,600	3,500	3,300					
SH25	2,000	900	2,100	800	900	900	600	1,000	4	3,300				
HIT32	300	1,100	1,100	2,100	1,200	1,000	1,300	1,100	1,900	4,500	1,900			
YAM32	1,000	300	1,300	1,300	600	300	500	500	1,000	3,900	1,000	900		
KM40	3,900	2,800	3,900	2,200	2,700	2,800	2,500	2,800	1,900	2,500	1,900	3,800	2,900	
KSJ	1,300	600	1,800	1,400	100	200	400	200	800	3,400	2,700	1,200	500	2,700

* The unit is (km). Each value is rounded off to the (nearest) 100. MIZ=VERA-Mizusawa; IRK=VERA-Iriki; OGA=VERA-Ogasawara; ISG=VERA-Ishigakijima; KYS=KVN-Yonsei; KUS=KVN-Ulsan; KTN=KVN-Tamna; KPC=KVN-Pyeongchang; TM65=TMRT65; NS26=NSRT26; SH25=SHRT25; KM40=KMRT40; KSJ=Sejong22.

4.2.7 An accurate delay model for astrometry

The initial delay tracking model used by KJCC correlator is not sufficient for high precision position measurement (i.e., astrometry). Therefore, we provide a calibration table (called the delay re-calculation table) to PIs, where the difference between the correlator model and an accurate model is written in the calibration table. The accurate model can take into account the latest station coordinates, accurate source (i.e., target) coordinates, the most-updated Earth Rotation Parameters (EOPs), tropospheric and ionospheric delays (see [23] for details). The calibration table can be loaded with the AIPS task `TBIN`.

In order to receive the calibration table for astrometry data reduction, PI can contact EAVN help, `eavnhelp(at mark)kasi.re.kr`. The delivery of observation data and calibration table will take about three months after the observation.

Necessary files including the information of delay and rate for epoch, which will be used at the Mizusawa correlation center, should be sent via e-mail to the EAVN User Support Team (`eavnhelp(at mark)kasi.re.kr`) or be uploaded on online cloud servers.

- List of the observation codes/epochs ayyID[a-z], such as a2503b for the 2nd (b) EAVN observation (a) of the project ID (ID=03) in 2025 (yy=25).

- IF_MODEL (there are ANT.* files in this directory) for each epoch.

- HEADDER for each epoch.

- FITSGEN.cntl for each epoch.

- AIPS LISTR (optype 'scan') for each epoch.

- Correlation parameters (delay and rate) for all antennas in each epoch.

To receive the files, please follow the procedure summarized below.

1. Ask the KJCC staff (`kjcc(at mark)kasi.re.kr`)to provide IF_MODEL(ANT.*), HEDDER, and FITSGEN.cntl in the CODA file system.

2. Prepare the AIPS LISTR results to show frequency settings (optype 'scan').

3. Prepare the correlation parameters (delay and rate) as instructed below.

   - Login to the EAVN site (`https://radio.kasi.re.kr/main.php`) and open the "Feedback" page. If you cannot login to the "Feedback" page, contact with the KJCC (`kjcc(at mark)kasi.re.kr`).

   - Search for your observation by the Exp_code or title.

   - List the details of the observation. In the "Correlation Comment" section, correlation parameters are listed as shown below.

     ```
     site 1 MIZ -4.18865e-06 1.11676e-13 2023054071700.0000
     site 2 IRK -3.9935e-06 -3.7017e-13 2023054071700.0000
     site 3 OGA 8.92612e-06 -2.7562e-14 2023054071700.0000
     site 4 ISG -2.02715e-06 1.94503e-13 2023054071700.0000
     ```

```
site 5 KYS -2.97714e-06 5.1074e-14 2023054071700.0000
site 6 KUS 1.032936088e-06
site 7 KTN -8.78551e-06 -1.98778e-13 2023054071700.0000
site 8 MOP -2.04603e-07 2.74113e-13 2023054071700.0000
```

4. Send the above information to the EAVN User Support Team via e-mail (`eavnhelp(at mark)kasi.re.kr`) or online cloud servers.

4.2.8 2B calibration table

In addition to the delay tracking model, it is necessary to apply the 2B calibration tables for the VERA dual-beam phase-referencing analysis. **If the VERA dual-beam phase-referencing data are correlated with the KJCC, please request the 2B calibration tables as well.** In the case of the fast antenna switching with VERA, the 2B calibration signal is not used in the observations and hence, the tables cannot be produced.

4.2.9 Data Reduction

Generally, users are encouraged to carry out data reduction in consultation with contact person and/or support scientist in the KaVA/EAVN project group. Procedure of astrometric data reduction for VERA data has been summarized in previous papers (e.g. Fig. 11 in [13]; Fig. 5 in [12]). Basically, the procedure of data reduction for KaVA/EAVN data is consistent with that for VERA data, expect for few points.

For instance, parallactic angle should be corrected if the fast switching observation is conducted with single beam. The NRAO AIPS task "CLCOR" can be used for the calibration by setting the OPCODE = "PANG".

4.2.10 Reference and Acknowledgment

Details of the recalculations, in which zenith troposphere delay, ionosphere delay, earth rotation parameter, station coordinate, and source coordinate are applied, should be referred to [17] in the published papers.

4.3 1-beam Hybrid (K/Q/W) Mode

KaVA will enable us to conduct VLBI observations in combinations of different types of antennas (antenna beams), receiving bands, recording rates (namely total band widths), and filtered base band channels in one observing session, whose cross correlation is still valid for the whole or some parts of KaVA. In such "hybrid" observing modes with KaVA, there are some modes that are available in the 2025A CfP described as follows.

Although VERA shall use only one of dual beams in a single frequency band (K or Q), the KVN is able to observe in two to three of K/Q/W bands simultaneously in a common observing session. Please check the KVN status report for W-band information:

```
https://radio.kasi.re.kr/status_report/status_report.php?site=kvn
```

Signal correlation for all the KaVA baselines is valid for the band in which both the KVN and VERA observe, while that for all the observed bands is valid for the KVN baselines.

Frequency allocations should be made separately to the KVN and VERA, including base band channels that are common between the two arrays in a specific band (K or Q). Note that the number of base band channels or the total bandwidth available per frequency band is limited, therefore brighter continuum sources should be selected for group-delay calibration.

4.4 Wide-field Imaging Mode

This mode is required to fully image 44 GHz methanol maser emissions associated with star-forming regions, which are generally distributed on the angular scale over 10 arcsec. The wide-field imaging (WFI) mode is achieved with an accumulation period shorter than the usual one of 1.6384 sec in Daejeon correlator at KJCC. Theoretically, the field of view (FoV) within an amplitude loss of 1%, 5%, and 10% is estimated on the basis of the time-average smearing effect due to a finite accumulation period [28]. The FoVs calculated for accumulation periods of 0.2048, 1.6384, and 3.2768 sec are summarized in Table 24, in the case of the highest angular resolution at Q-band of 0.6 mas with KaVA.

Table 24: FoV within a given amplitude loss in each accumulation period[*].

	Amplitude loss		
	1.0%	5.0%	10.0%
Accumulation period	FoV	FoV	FoV
(sec)	(arcsec)	(arcsec)	(arcsec)
0.2048	8.6	19.4	27.4
1.6384	1.1	2.4	3.4
3.2768	0.5	1.2	1.7

* Under an assumption of the highest angular resolution at Q-band of 0.6 mas with KaVA.

In the current available specification of Daejeon correlator, there is a trade-off between a shorter accumulation period and a larger number of IF channels to yield higher spectral resolution. The most highly recommended setup is the combination of C2 mode and an accumulation period of 0.2048 sec, in which both a sufficiently high velocity resolution (0.11 km s^{-1} for 44 GHz methanol masers) and a sufficiently wide FoV (10 arcsec or more) can be obtained. Thus the recommended set-up for WFI mode is summarized in Table 25.

Table 25: Recommended set-up for WFI mode in the current situation.

Correlation mode	Sampling rate	Bandwidth /IF	Accumulation period	Spectral channels/IF
C2	1024 Mbps	128 MHz	0.2048 sec	8,192

The evaluation for the WFI tests was done by the following two ways: comparing the

data of an accumulation period of 0.1 sec produced in DiFX to those of 0.2048 sec in Daejeon correlator, and comparing the latter data to the same data but with averaging in 3.2768 sec. These ways provide us a chance to estimate whether such an isolated maser can be detected or not and how much rate of the amplitude loss occurs. The evaluation might be updated on the basis of a comparison between a short-accumulation period data and a multi-tracking center data in the near future.

If you would like to require this WFI mode, please describe your requests in the following two items:

- Requested setting parameters for WFI in the proposal cover sheet

- Reasons for requiring WFI mode in the scientific justification

Finally, note that the file size of correlated data for WFI is as huge as ~600 GByte. We therefore recommend to check and improve the performance of your internet environment and personal computer as high as possible for comfortable data downloading and data processing, respectively. Please refer an example parameters in Table 26:

Table 26: Required performances of internet and personal computer.

Forward speed	≥ 10 MByte s^{-1}
HDD/SSD volume	≥ 1.5 TByte
RAM	≥ 16 GByte

Here, the experiment to verify the time-average smearing effect due to a finite accumulation period has been done, however we will also verify the bandwidth smearing effect to KaVA observations in the near future.

4.5 Simultaneous K/Q Band Mode

Simultaneous K/Q-band data reception mode is available for KaVA, NRO45, and KSJ on a limited basis for open-use. Please note the following limitation: (1) K/Q simultaneous observations cannot be performed regularly but will be performed by setting up to two sessions in 2025A semester (where each slot spans approximately one–two week(s)) because VERA requires a special setup at the front-end for K/Q simultaneous reception. **The term of K/Q session will be determined depending on requests shown in proposals submitted. Although proposers are eligible to specify an appropriate date or term for their observations in the proposal, the request is not always accepted. Monitoring project using the K/Q system will not be accepted for the 2025A semester.** (2) The frequency setup is fixed as shown in Table 27. Especially when NRO45 joins, the frequency setup is strictly limited as in Table 27. The term of K/Q session will be determined depending on requests of approved proposals. (3) Frequency phase transfer (FPT) technique [27] is not applicable to the data obtained at NRO45. (4) 'Template method' for the amplitude calibration should be employed to the data obtained at NRO45 since the system noise temperature cannot be measured using the K/Q-band simultaneous reception system at Nobeyama. (5) **Multi-frequency mode and dual-polarization mode cannot be employed simultaneously for the EAVN session in the 2025A semester.**

Table 27: Frequency setup for simultaneous K/Q band observation

Band	Frequency range	BBC channel	Polarization
Without NRO45			
K-band	22.112 - 22.240 GHz	32 MHz x 4 channels	**RCP**
Q-band	42.812 - 42.940 GHz	32 MHz x 4 channels	**LCP**
With NRO45			
K-band	22.116 - 22.244 GHz	16 MHz x 8 channels	**RCP**
Q-band	42.816 - 42.944 GHz	16 MHz x 8 channels	**LCP**

A demonstrative observation and detailed performance of simultaneous K/Q-band observations with KaVA is presented in the Zhao et al. (2019). You can also check science cases with simultaneous multi-frequency VLBI observations [7].

4.6   Condition on the Usage of Nobeyama 45-m Telescope

In the 2025A semester, NRO 45-m telescope will not join the EAVN observations due to the problem in the hydrogen maser operated by the Mizusawa VLBI Observatory of NAOJ.

5 Observation and Data Reduction

5.1 Preparation of an EAVN Observation

You will be notified when your observation is scheduled by the EAVN scheduling officer. After the acceptance of proposals, users are requested to prepare the observing schedule file. Information about the user support is available at the EAVN web site:

https://radio.kasi.re.kr/eavn/user_support.php

Your schedule file must be submitted to `eavnobs@kasi.re.kr` <u>two weeks</u> **before your observing date. If your schedule submission is delayed, your observation may not be assigned.** For the EAVN schedule submission, PI should submit both a stand-alone vex file and a SCHED key file. In the vex file, please specify calibration procedures for hot/cold calibration, sky dipping, pointing, etc. We also request PIs to specify your correlation parameters at the beginning of the vex file (in case of EAVN observation) or in the key file (in case of KVN observation) for proper correlation processing. In particular, PIs who request for sub-array or dual-beam observations for EAVN should provide a frequency matching table for the correct correlation.

On your schedule, we strongly recommend to include at least two fringe finder scans, each lasting 5 or more minutes at the first and latter part of observation in order to search the delay and rate offsets for the correlation.

For EAVN which includes the large telescopes (TMRT65 and NRO45), regular pointing check is necessary at both K- and Q-bands. You should leave a $8 - 15$ min gap every $\leq 1 - 2$ hr in your schedule file to allow this. Pointing check is done by the local operators. In addition, we strongly recommend to include frequent scans of a maser source and/or a bright compact continuum source located within $15°$ from the target. This allows a cross check of the amplitude calibration for TMRT65 and NRO45 along with the usual a priori method.

If you request the participation of the YAM32 and/or KMRT40 and/or NSRT26 antennas at C-band, it is mandatory to do gain calibration and absolute flux scaling by the template spectrum method. In this method, a strong and compact CH_3OH maser source that locates within $15°$ from the target source is observed with an interval of 1 hr or shorter. In particular during elevations lower than $20°$, it is recommended to observe these calibrators every 30 min or shorter. Even if the YAM32 and/or KMRT40 and/or NSRT26 antennas are not included, it is recommended to observe the strong and compact CH_3OH maser source with the same interval as the cross-check for the gain curve and absolute flux scaling of the TMRT65 antenna as well. To select calibrators appropriated to your target sources, please see Section 3.10.

In the case of any observations for CH_3OH masers at 6.7 GHz in C-band, it is strongly recommended to request the C5 correlation mode (16 MHz $\times$ 16 IFs) and the maximum spectral channels 8,192 for IF5 including the maser emission (corresponding to RF 6,664–6,680 MHz with the normal frequency set-up) to achieve the sufficient channel resolution of 1.953 kHz, yielding to the velocity resolution of $\sim$0.088 km s^{-1}.

For NRO45, TAK32, HIT32, and YAM32, only fixed frequency settings (i.e., RF ranges and DFU modes) can be accepted to process the DFU copy in the NAOJ Mizusawa correlation center (Sections 2.4 and 2.4.1). For

observations using either NRO45, TAK32, HIT32, and/or YAM32, digital filter settings of the sample schedule files provided on the EAVN website should not be changed. For the C-band observations (HIT32 and YAM32), the frequency setting (RF range) cannot be changed, as listed in Table 8. For the K-band observations (NRO45 and/or TAK32), fixed RF ranges are strongly recommended, as listed in Table 8. If user-specified frequency settings at K-band are required, please consult with the EAVN User Support Team (UST) well in advance. In order to confirm the DFU copy process, we ask the observers to include at least one scan of a strong maser source (at the 1st scan, if possible). When the scan for the maser source is included, it should be commented (either the maser source or the scan number) in the vex file.

5.1.1 Sample Key Files for NRAO sched

From the 2023A semester, EAVN UST provides sample key files to be used for preparation of schedule files. Basic information and user guide are available on the EAVN website:

$$\text{https://radio.kasi.re.kr/eavn/user\_support.php}$$

There are collection of the inputs for the NRAO sched software. Files are available on the same EAVN website. For more details of NRAO sched, please refer to the NRAO website as listed in the above website. The above sample key files take into account special settings optimized to EAVN observations (e.g. fixed/nominal frequency setting recommended/required for each telescope). Thus, the EAVN users are strongly recommended to use the above sample key files. The detailed information will be updated on the EAVN website.

5.1.2 EAVN Stations and Locations Files for NRAO sched

Information on each EAVN station is updated regularly, so it is strongly recommended that users use the latest version of the stations and locations files, which are available on the '3. SCHED for EAVN' on the EAVN User Support page (linked above). When running SCHED, these two files should be moved to your `$SCHED/catalogs/` directory. This will help to avoid the observation failure at a particular antenna, and reduce the additional effort required by the UST to correct the submitted vex file. The officially used EAVN station names and codes for SCHED are listed in Table 28.

5.2 Observation and Correlation

EAVN members take full responsibility for observation and correlation process, and thus basically proposers will not be asked to take part in observations or correlations. Observations are proceeded by operators from each array and telescope, and correlated data is delivered to the users in approximately two months including the time for media shipping to KJCC at Daejeon.

Table 28: EAVN station names and codes for running SCHED

SITE in this report	STATION NAME in SCHED	STATION CODE in SCHED
KVN-Yonsei (KYS)	KVNYS	Ky
KVN-Ulsan (KUS)	KVNUS	Ku
KVN-Tamna (KTN)	KVNTN	Kt
KVN-Pyeongchang (KPC)	KVNPC	Kc
VERA-Mizusawa (MIZ)	VERAMZSW	Vm
VERA-Iriki (IRK)	VERAIRIK	Vr
VERA-Ogasawara (OGA)	VERAOGSW	Vo
VERA-Ishigakijima (ISG)	VERAISGK	Vs
Nobeyama 45-m (NRO45)[a]	NRO45	Ny
Takahagi 32-m (TAK32)	TAKAHAGI	Tk
Hitachi 32-m (HIT32)	HITACHI	Ht
Yamaguchi 32-m (YAM32)	YAMAGU32	Ym
Tianma 65-m (TMRT65)	TIANMA65	T6
Sheshan 25-m (SHRT25)	SHANGHAI	Sh
Nanshan 26-m (NSRT26)	URUMQI	Ur
Kunming 40-m (KMRT40)[a]	KUNMING	Km
Sejong 22-m (KSJ)	SEJONG	Kv

[a]Will not participate in the 2025A

After the correlation, the user will be notified where the data can be downloaded by e-mail. After one month later of a correlated data distribution to PIs, disk modules which contains raw observing data can be recycled without notice. Therefore, PIs should investigate the correlated output carefully. For re-correlation or raw data keeping of the data, PI should provide adequate evidence in order to justify his/her request. If there is an issue related to correlated data, PI should contact with the EAVN UST or the correlator team (`kjcc (at-mark) kasi.re.kr`), and not to ask KJCC members directly.

5.3 Data Reduction

For EAVN data reduction, the users are encouraged to reduce the data using the NRAO AIPS software package. The observation data and calibration data will be provided to the users in a format which AIPS can read.

As for the amplitude calibration, we will provide "ANTAB" files which include the system temperature information measured by the R-sky method and the information of the dependence of aperture efficiency on antenna elevation, except YAM32 and KMRT40 antennas where the gain calibration and absolute flux scaling have to be achieved via the template spectrum method in the AIPS task "ACFIT". A sample script for the template spectrum method is available on the EAVN website (see section 5.3.1). If the user needs weather information, the meteorological data of the temperature, pressure, and humidity during the observation can be provided.

5.3.1   Sample AIPS Recipes

EAVN UST will provide sample recipes for data calibration and imaging by using AIPS. These are simple script files for the following observation settings:

- KaVA observation of the 22 GHz H_2O maser

- EAVN observation of the 6.7 GHz CH_3OH maser

- EAVN phase-referencing observation at K-band

- RUN file for the KaVA phase-referencing astrometry of the 22 GHz H_2O maser

A sample script for the amplitude calibration procedure via the template spectrum method is available. Files are available the following EAVN web sites:

https://radio.kasi.re.kr/eavn/user_support.php

While these files cover only widely used basic setting but not all the available observation modes, they can be modified for your observation mode.

5.3.2   Additional Tables for phase-refereceing observations

Some additional files are required in the case of phase-referencing observations, such as the accurate delay tracking models and VERA dual-beam calibration tables. Details of these additional information are summarized in Sections 4.2.7, 4.2.8, and 4.2.10.

5.4   Policy of User Support

EAVN will not assign any support scientists to all the accepted proposals. If the proposers/observers have any inquiry about EAVN observations, they should contact with the EAVN UST and/or the relevant addresses as listed in Table 29. If the proposers need extensive support by the EAVN experts for schedule preparation and data analysis, they can request to assign a support scientist in the proposal cover sheet. UST will arrange the support scientist to the accepted proposals which request extensive support considering their science cases and its necessity.

5.5   Acknowledgment

All EAVN users (both proposers for using EAVN and data analysts using EAVN archive data) are asked to specify the following acknowledgment (or similar one) to EAVN in their publications.

This work is made use of the East Asian VLBI Network (EAVN), which is operated under cooperative agreement by National Astronomical Observatory of Japan (NAOJ), Korea Astronomy and Space Science Institute (KASI), Shanghai Astronomical Observatory (SHAO), Xinjiang Astronomical Observatory (XAO), Yunnan Astronomical Observatory (YNAO), National Astronomical Research Institute of Thailand (Public Organization) (NARIT), and National Geographic Information Institute (NGII), with

the operational support by Ibaraki University (for the operation of Hitachi 32-m and Takahagi 32-m telescopes), Yamaguchi University (for the operation of Yamaguchi 32-m telescope), and Kagoshima University (for the operation of VERA Iriki antenna).

Please include participating telescopes of your project in Acknowledgment of your publications.

5.6 Further Information

The users can contact any staff member of EAVN by e-mail (see Table 29).

Table 29: Contact addresses.

Name	E-mail address*	Related Field
Inquiry about proposal submission	eavnprop	Proposal-related requests/questions
User support team	eavnhelp	User support in general, request for recalculation of correlator model (phase-referencing)
Operation team	eavnobs	Observation-related requests/questions, schedule submission
Correlator team	kjcc	Correlation-related requests/questions, correlated data distribution

∗: Add @kasi.re.kr to the address.

References

[1] EAVN Status Report for the 2025A Semester:
https://radio.kasi.re.kr/status_report.php?cate=EAVN

[2] KVN Status Report:
https://radio.kasi.re.kr/status_report.php?cate=KVN

[3] NRO web site:
http://www.nro.nao.ac.jp/~nro45mrt/html/index-e.html

[4] Akiyama, K. et al. 2022, Galaxies, 10, 113

[5] Cho, I. et al. 2017, PASJ, 69, 87

[6] Cui, Y. Z. et al. 2021, RAA, 21, 205

[7] Dodson, R. et al. 2017, ApJ, 834, 177

[8] Hachisuka, K. et al. 2006, ApJ, 645, 337

[9] Han, S.-T. et al. 2008, Int. J. Infrared Millimeter Waves, 29, 69

[10] Han, S.-T. et al. 2013, PASP, 125, 539

[11] Honma, M. et al. 2008, PASJ, 60, 951

[12] Imai, H. et al. 2012, PASJ, 64, 142

[13] Kurayama, T. et al. 2011, PASJ, 63, 513

[14] Lee, S.-S. et al. 2015, JKAS, 48, 229

[15] Martí-Vidal, I. et al. 2010, A&A, 515, 53

[16] Nagayama, T. et al. 2015, PASJ, 67, 65

[17] Nagayama, T. et al. 2020, PASJ, 72, 52

[18] Oh, S.-J. et al. 2011, PASJ, 63, 1229

[19] Okada, T. et al. 2020, PASJ, 71, 7

[20] Ott, M. et al. 1994, A&A, 284, 331

[21] Oyama, T. et al. 2016, PASJ, 68, 105

[22] Reid, M. J. & Honma, M. 2014, ARA&A, 52, 339

[23] Sakai, N. et al. 2023, PASJ, 75, 208

[24] Wajima, K. et al. 2016, ASPC, 502, 81

[25] Yonekura, Y. et al. 2016, PASJ, 68, 74

[26] Yoo, S. M. et al. 2018, JKAS, 51, 143

[27] Zhao, G. Y., et al. 2019, JKAS, 52, 23

[28] Proceedings from the 1988 synthesis imaging workshop in NRAO, Chapter 13 in Synthesis Imaging in Radio Astronomy: A Collection of Lectures from the Third NRAO Synthesis Imaging Summer School:
http://www.aspbooks.org/a/volumes/table_of_contents/?book_id=118